Keratin building blocks from feathers for material applications

Emmi-Maria Nuutinen

Aalto University

Keratin building blocks from feathers for material applications

Emmi-Maria Nuutinen

A doctoral thesis completed for the degree of Doctor of Science (Technology) to be defended, with the permission of the Aalto University School of Chemical Engineering, at a public examination held at the lecture hall Ke2 of the school on 7th October 2022 at 13 o'clock.

Aalto University
School of Chemical Engineering
Department of Bioproducts and Biosystems
Bioproduct Chemistry

Supervising professor
Professor Monika Österberg, Aalto University, Finland

Thesis advisor
Doctor Stina Grönqvist, VTT Technical Research Centre of Finland, Finland

Preliminary examiners
Professor Wim Thielemans, KU Leuven, Belgium
Professor Chris Carr, University of Leeds, United Kingdom

Opponent
Doctor Koon-Yang Lee, Imperial College London, United Kingdom

NORDIC SWAN ECOLABEL

Printed matter
4041-0619

Abstract

Feathers, a byproduct of the poultry industry, are a rich source of keratin. Thus, the valourization of feathers is highly relevant, considering the aspects of resource sufficiency and the circular economy. This doctoral thesis aimed to convert feathers into keratin building blocks and evaluate their utilization in material applications. Keratin as a structural protein has interesting properties, considering applications in the medical, cosmetics, electronics, agriculture, textile and composite industries. To produce molecular keratin, feathers were dissolved in an aqueous deep eutectic solvent (DES). It was found that the DES used was able to disturb the interactions within the feather keratin, cleave the disulfide bonds, alter the conformation and partially break down the polypeptide backbone, and that the molecular weight of the keratin played an important role in its solubility. Film structures were prepared from molecular keratin to study the physical properties and reactivity of keratin. The conformation and molecular weight of keratin, as well as the addition of plasticizers and cross-linkers, had determinant roles in the mechanical properties and water sensitivity of the films. To compare the used DES process to a mechanical treatment, a simpler alkaline pre-treatment combined with milling was carried out to produce fibrous keratin. A comparison of films made of molecular and fibrous keratin showed that fibrous keratin is suitable in applications such as composites, in which transparency, good barrier properties or reactivity are not required, while molecular keratin is suitable in various applications. To evaluate the possibility to combine keratin with other bio-based materials, the adsorption of keratin peptides obtained from the used DES process on cellulose and lignin substrates was studied. The interactions between cellulose and keratin peptides were found to be weak, while on lignin substrates, keratin peptides had high adsorption. The structural properties of keratin—including the amino acid content, molecular weight, and random coil conformation together with the negative net charge of lignin surfaces—were demonstrated to be the determinanting factors in for the adsorption behaviour. In particular, the combination of colloidal lignin particles and keratin is interesting, as the spherical morphology of the nanoparticles is beneficial in many practical applications. Overall, the thesis furthers our understanding of how the choice of the processing method affects the structural and physical properties of the feather keratin as well as its interactions with lignocellulosics. These are important for the utilization of keratin in macro- and nanoscale material applications.

Tiivistelmä

Höyhenet, siipikarjateollisuuden sivutuote, ovat erinomainen keratiinin lähde, ja niiden hyödyntäminen on olennaista resurssien riittävyyden ja kiertotalouden näkökulmasta. Tämän väitöskirjan tavoitteena oli arvioida höyhenkeratiinin sopivuutta materiaalisovelluksissa. Proteiinina keratiinilla on mielenkiintoisia ominaisuuksia, joita voi hyödyntää esimerkiksi lannoitteissa, palonestoaineissa, imeytysaineissa sekä biolääketieteen, kosmetiikan ja elektroniikan sovelluksissa. Molekyylistä keratiinia valmistettiin liuottamalla höyheniä vesipitoiseen syväeutektiseen liuottimeen (DES:iin). Käytetty DES muutti keratiinin vuorovaikutuksia, katkaisi disulfidisidoksia, muokkasi konformaatiota ja osittain hajotti polypeptidirunkoa. Keratiinin molekyylipainolla havaittiin olevan tärkeä rooli sen liukoisuudessa. Liukoisuuden lisäksi keratiinin molekyylipainolla ja konformaatiolla oli tärkeä rooli keratiinista valmistettujen kalvorakenteiden mekaanisissa ominaisuuksissa sekä vesivuorovaikutuksissa. Näitä ominaisuuksia voitiin kuitenkin kontrolloida myös lisäämällä kalvorakenteeseen pehmittimiä ja silloitusaineita. DES-prosessin lisäksi höyheniä prosessoitiin yksinkertaisemmalla mekaanisella käsittelyllä kuitumaisen keratiinin tuottamiseksi. Molekyyli- ja kuitukeratiinista valmistettujen kalvorakenteiden vertailusta todettiin, että kuitukeratiini sopii sovelluksiin, joissa läpinäkyvyys, hyvät läpäisevyysominaisuudet tai reaktiivisuus eivät ole olennaisia kuten komposiiteissa, kun taas molekyylikeratiini soveltuu moniin erilaisiin sovelluksiin. Keratiinin molekyylipainon tärkeys havaittiin myös, kun tutkittiin DES-prosessoitujen keratiinipeptidien adsorptiota selluloosa- ja ligniinisubstraatille. Selluloosan ja keratiinipeptidien välisten vuorovaikutusten havaittiin olevan heikkoja, kun taas ligniinisubstraateille keratiinipeptideillä oli korkea adsorptio. Keratiinin rakenteellisten ominaisuuksien, mukaan lukien molekyylipaino, aminohappokoostumus ja satunnainen konformaatio sekä ligniinin negatiivinen varaus, huomattiin olevan tärkeässä roolissa keratiinin adsorptiossa ligniinipinnoille. Erityisesti kolloidiset ligniinihiukkaset keratiinin kanssa ovat mielenkiintoinen mahdollisuus, koska nanohiukkasten pallomainen morfologia on hyödyllinen monissa käytännön sovelluksissa, kuten hydrogeeleissä. Kaiken kaikkiaan saadut tulokset parantavat ymmärrystämme siitä, kuinka käsittelymenetelmän valinta vaikuttaa höyhenkeratiinin rakenteellisiin ja fysikaalisiin ominaisuuksiin sekä sen vuorovaikutuksiin lignoselluloosan kanssa.

Acknowledgements

First of all, I would like to thank my supervising professor, Monika Österberg, who has been a permanent part of my journey to complete my doctoral studies. Your support has been one of the most sustaining forces, and I appreciate all the things I have learned from you.

Next, I would like to thank Dr Anna-Stiina Jääskeläinen, who encouraged me in doctoral studies and acted as my advisor at the beginning. You are one of the most inspiring persons I know, and I am grateful that our communication has continued, even though we now work in different places. I want to thank Dr Raija Lantto for taking me under her guidance after Anna-Stiina left VTT. You taught me a lot about more than just doing science. Next, I want to thank my advisor and current manager, Dr Stina Grönqvist, who stepped in to help and support me when I needed it the most to complete my studies. I really appreciate your way of getting things done. I would like to thank Dr Tekla Tammelin whose professional approach, especially at the end, was highly appreciated, and my former manager Dr Tiina Liitiä for your support at the beginning of my studies.

I want to thank all my co-authors: Dr Mika Vähä-Nissi, Dr Pia Willberg-Keyriläinen, Dr Tommi Virtanen, Professor Alice Mija, Dr Lauri Kuutti, Dr Juan José Valle-Delgado, Dr Miriam Kellock, Dr Muhammad Farooq, Tiina Pöhler, Timo Kaljunen and Panu Lahtinen for their fruitful collaboration and expertise. I would like to thank Päivi Matikainen for her priceless help and support in the lab. For mental support, I want to thank my current and former colleagues Olesya, Miriam, Jenni, Ilona, Piritta, Saara and Riina.

I want to thank all my dear friends for the good times in my free time. I am grateful to be surrounded by so many great people whom I can call friends. Special thanks to Kata, who has been there whenever I needed a friend the most.

Finally, my greatest thanks go to äiti, isi and Sanna. I am extremely grateful that we have such a loving and supportive family.

Helsinki, July 2022
Emmi-Maria Nuutinen

Contents

List of Abbreviations and Symbols

Arg	Arginine
Asp	Asparagine
ATR	Attenuated total reflectance
BDE	1.4-butanediol diglycidyl ether
CD	Circular dichroism
CLP	Colloidal lignin particles
CLSM	Confocal laser scanning microscopy
Cys	Cysteine
DES	Deep eutectic solvent
FTIR	Fourier transform infrared spectroscopy
GA	Glutaraldehyde
Glu	Glutamine
Gly	Glycine
IEP	Isoelectric point
IL	Ionic liquid
Leu	Leucine
MALDI-TOF	Matrix-assisted laser ionization time of flight
MS	Mass spectrometry
Mw	Molecular weight
NMMO	N-methylmorpholine N-oxide
NMR	Nuclear magnetic resonance spectroscopy
PI	Polydispersity index
Pro	Proline
QCM-D	Quartz crystal microbalance with dissipation monitoring
RH	Relative humidity

SAB	Sodium acetate buffer
SEC	Size exclusion chromatography
SEM	Scanning electron microscopy
Ser	Serine
SPB	Sodium phosphate buffer
TMSC	Trimethylsilyl cellulose
Val	Valine
WCA	Water contact angle
WVP	Water vapour permeability
WVTR	Water vapour transmission rate
XRD	X-ray diffraction analysis
ΔG_m	Free energy
M_n	Number average molecular weight
M_w	Weight average molecular weight
θ_{eq}	Contact angle
ΔD	Dissipation change
Δf	Frequency change
χ	Flory interaction parameter

List of Publications

This doctoral dissertation consists of a summary and the following publications, which are referred to in the text by their numerals.

I Nuutinen, Emmi-Maria; Willberg-Keyriläinen, Pia; Virtanen, Tommi; Mija, Alice; Kuutti, Lauri; Lantto, Raija; Jääskeläinen, Anna-Stiina. 2019. Green process to regenerate keratin from feathers with an aqueous deep eutectic solvent. Royal Society of Chemistry. RSC Advances, 9, 34, 19720-19728. DOI: 10.1039/C9RA03305J.

II Nuutinen, Emmi-Maria; Virtanen, Tommi; Lantto, Raija; Vähä-Nissi, Mika; Jääskeläinen, Anna-Stiina. 2021. Ductile keratin films from deep eutectic solvent-fractionated feathers. Royal Society of Chemistry. RSC Advances, 11, 44, 27512-27522. DOI: 10.1039/D1RA05123G.

III Nuutinen, Emmi-Maria; Valle-Delgado, Juan José; Kellock, Miriam; Farooq, Muhammad; Österberg, Monika. Affinity of keratin peptides for cellulose and lignin: a fundamental study toward advanced bio-based materials. Langmuir, Publication Date: August 5, 2022. DOI: 10.1021/acs.langmuir.2c01140.

IV Vähä-Nissi Mika; Lahtinen, Panu; Nuutinen, Emmi-Maria; Kaljunen, Timo; Pöhler, Tiina. Films from an aqueous suspension of alkaline pretreated and fine milled chicken feathers. Scientific Research Publishing. Materials Sciences and Applications, 11, 1, 27-43. DOI: 10.4236/msa.2020.111003.

Authors' Contributions

Publication I: Green process to regenerate keratin from feathers with an aqueous deep eutectic solvent

EMN had the main responsibility for planning, managing and carrying out the experimental work as well as writing the manuscript together with ASJ, LK and RL. PWK carried out the DSC measurements and analysed the results together with EMN. TV carried out the NMR measurements and analysed the results together with EMN. XRD measurements and the result analysis were done under the supervision of AM.

Publication II: Ductile keratin films from deep eutectic solvent-fractionated feathers

EMN had the main responsibility for planning and carrying out the experimental work as well as writing the manuscript together with ASJ, RL and MVN. TV carried out the NMR measurements and analysed the results together with EMN.

Publication III: Adsorption of keratin peptides on cellulose and lignin: a fundamental study toward advanced bio-based materials

EMN had the main responsibility for planning, carrying out the experimental work and writing the manuscript under the supervision of MÖ and other co-authors. JJVD supported EMN to carry out the QCM-D measurements and AFM imaging. MK gave her support especially in keratin characterization. FM was especially helpful in the preparation of lignin thin films and the graphical illustration of the manuscript.

Publication IV: Films from an aqueous suspension of alkaline pretreated and fine milled chicken feathers

EMN planned and reported the work together with the co-authors. MVN had the main responsibility for planning, carrying out the experimental work and writing the manuscript. The work was part of the project in which EMN had the main responsibility.

1. Introduction and aims

We need to create new, cost-competitive, bio-based materials that can address the main challenges of our century, which include resource sufficiency and climate change. In 2020, the global annual production of plastics and synthetic fibres were 367 and 74 million metric tons, respectively.[1,2] This opens up huge opportunities for new sustainable and advanced bio-based material solutions to enter the markets to replace conventional fossil-based products. Lignocellulosic building blocks are currently being studied extensively to replace fossil-based ones. But realizing the needed volumes and the required properties, we cannot exclude other bio-based alternatives, like proteins, as building blocks for future materials.

One of the most underutilized protein sources is the feather side stream of the poultry industry. In 2020, it was estimated that the poultry industry generated 13.6 million tons of meat in the European Union (EU)[3], which is approximately 2 million tons of feather waste annually just in the EU[4]. Although feathers contain about 90% of a protein called keratin, these feathers are mostly either burned, buried in landfills or recycled as poorly digestible feed, leaving about 1.8 million tons of protein to be used in higher-value products.[5,6] For comparison, the average pulp mill produces about 0.24 million tons of pulp annually.[7]

One of the reasons that limits the commercial use of feather keratin is the strong and complex structure of the feathers. Feathers can rarely be utilized without any processing. As feathers are resistant to the majority of chemical and physical conditions, their processing, and thus the utilization of feather keratin, is difficult.[5,8] Hence, feasible processing methods to convert feathers into a useful form should be developed. Moreover, to maximize the value addition for feather keratin, the most suitable applications should be identified. This kind of identification requires a deep understanding of keratin and how its structure and interactions are linked to its properties.

Feather keratin, when processed in a sustainable and feasible manner, not only could it bring additional value to bio-based materials, especially in the biomedical, cosmetology, packaging, and textile industries, but could also serve the principles of the circular economy through waste valourization. The aim of the thesis was to understand how feathers could be converted into utilizable keratin fractions and evaluate their potential as building blocks for future materials (Figure 1). More specifically, the thesis aims to meet the following objectives:

- Generate molecular and fibrous keratin building blocks from the feather sidestream via sustainable physical and chemical routes
- Understand the processability and chemical structure of molecular keratin building blocks by studying feather processing with an environmentally friendly aqueous deep eutectic solvent
- Explore the potential of molecular and fibrous keratin building blocks as self-standing film structures and understand the mechanical properties of these structures, their interaction with moisture and the effect of additives
- Recognize the opportunity to prepare combined materials by studying the interactions of keratin building blocks with cellulose and lignin
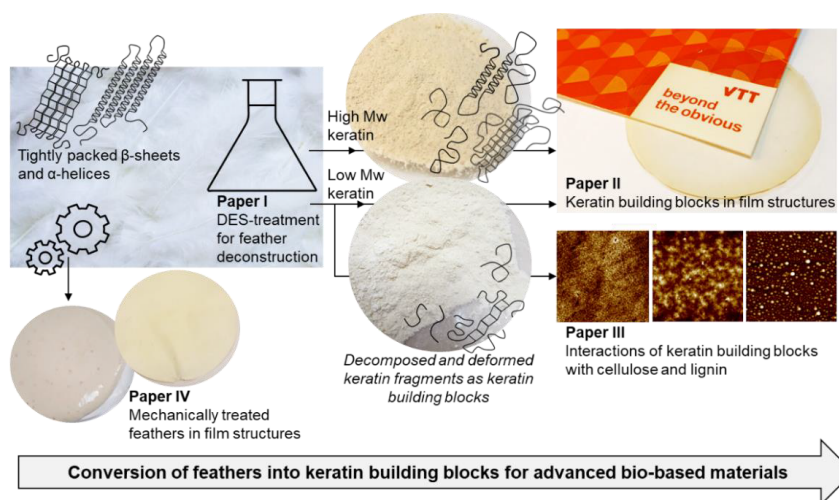
Figure 1. Schematic summary of the dissertation with the aim of exploring the potential of feather keratin as a building block for future materials.

The aim of **Publication I** was to define the molecular keratin building blocks prepared via a chemical route. The keratin building blocks were prepared by first dissolving the feathers in an aqueous deep eutectic solvent (DES) and using water to regenerate the dissolved keratin. After adding water, the keratin fraction with a higher molecular weight (Mw) distribution precipitated, while the keratin fraction with a lower Mw distribution remained soluble in water together with the diluted DES components. An extensive structural study of the high Mw keratin fraction was conducted to deduce its chemical structure.

In **Publication II**, high and low Mw keratin fractions were further used to prepare self-standing films to understand the effect of keratin structure and the effect of plasticizer and cross-linkers on the physical properties of keratin films.

In **Publication IV**, a simple alkaline pre-treatment and milling were used to prepare fibrous keratin building blocks via a mechanical route to recognize the advantages of molecular and fibrous keratin building blocks. More specifically, in **Publication IV**, the effect of different additives on film formation and the tensile properties of the fibrous keratin films was studied.

Publication III utilized a thin film approach to study the adsorption of DES-processed keratin peptides on lignocellulosic model films to obtain an understanding of how keratin can be integrated with other biomaterials for advanced material properties. A quartz crystal microbalance with a dissipation monitoring (QCM-D) technique revealed insights into the interactions between the keratin building blocks and lignocellulosic materials as well as the role of water in these interactions.

2. Background

2.1 Building blocks made of feather keratin

2.1.1 Feather keratin structure

Feathers are complex and hierarchical components as a result of biological evolution[9], and their main functions in nature include flight, camouflage, courtship, thermal insulation and water resistance.[10] In general, feathers have low density, good compressibility, and elasticity. They consist of two main structural units: rachis and barbs (Figure 2a). Rachis and barbs are both fibre-like structures with a hollow honeycomb structure (Figure 2b–f).[11,12] The study of feathers is difficult due to their robust hierarchical structure and variation between different keratin structures.[13,14]
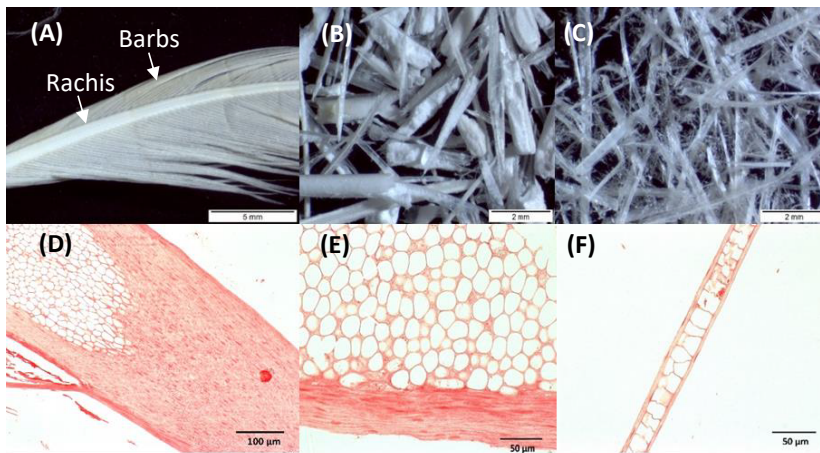
Figure 2. Overall appearance of (a) a feather, (b) ground rachis and (c) ground barbs, showing the inner honeycomb structure and fibrous outer layer, while Brightfield-imaged, diagonally cut and Ponceau S-stained (d,e) rachis and (f) barb show the structures of the inner honeycomb structure and fibrous outer layer in more detail.

Feathers consist of about 90% of a structural protein, keratin.[5] Keratin is a fibrous and tough protein.[10] Besides feathers, other materials, such as wool and hair, are also rich in keratin. Natural materials, which are rich in keratin, have a similar fibre-reinforced composite structure in which crystalline highly axially oriented intermediate filaments, microfibrils, are embedded in an amorphous and non-fibrous keratin matrix (Figure 3).[10,13–15]
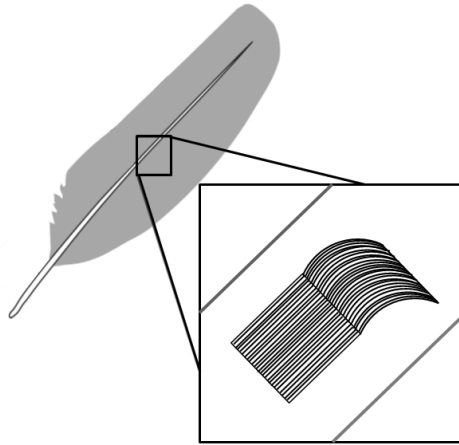
Figure 3. Keratin microfibrils embedded in an amorphous protein matrix.

Keratin, like all proteins, is made up of amino acid residues that are bonded by peptide bonds to form the main structure of the protein, a linear sequence of amino acids—polypeptides. Polypeptides have free amine and carboxylic acid groups at the ends of the polypeptide chains, also known as N- and D-terminal domains (Figure 4). Depending on the amino acid sequence, these polypeptides can form ordered secondary structures from which α-helix and β-sheet are the most common ordered conformations (Figure 5). In proteins, some polypeptides do not form an ordered and regular secondary structure; these regions are known as random coils.
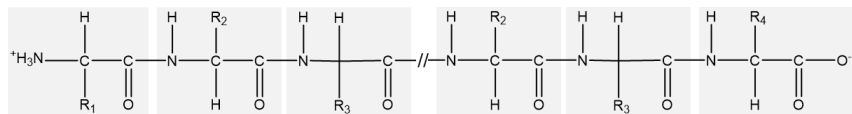
Figure 4. Amino acid residues linked by peptide bonds forming a primary structure of a protein. R is the side chain of an amino acid. The left end is the N-terminal domain, while the right end shows the D-terminal domain.
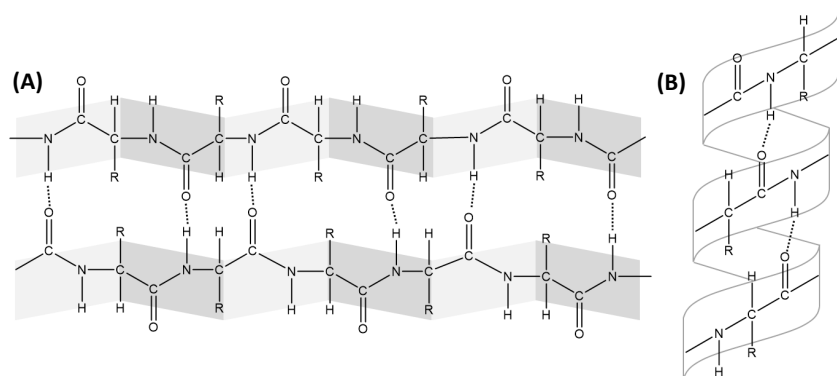
Figure 5. Polypeptides folded into the two most common ordered secondary structures: (a) β-sheets and (b) α-helix.

Although feather keratin has both ordered secondary structures, it is considered hard keratin, which means that the dominant secondary structure is β-sheet instead of α-helix.[10,14] It has been suggested that hard feather rachis have a higher content of β-sheets, while barbs have a higher α-helix content, thus indicating a softer keratin structure.[16] In keratin-rich materials, these ordered structures are especially located in the microfibrils, while the amorphous matrix consists mainly of unordered random coil keratin.[14,15] Furthermore, the central domain of feather keratin is associated with the microfibrils, while the N- and C-terminal domains are associated with the amorphous matrix. It is suggested that the central domain has amino acid residues that favour β-sheets, while the matrix is rich in amino acid residues related to the random coil conformation.[14,17,18] Overall, the complex filamentous hierarchy and the tight packaging of ordered secondary structures play an important role in the mechanical properties of feathers.[10,14,15]

It has been suggested that a single microfibril in a feather could consist of about 15–21 keratin polypeptide chains[19] and a single polypeptide chain extracted from a feather barb consists of 96 amino acid residues.[18] The amino acid sequence determines the properties and folding of the protein. In general, structural proteins such as keratin have a characteristic and repeating amino acid sequence that enables a higher-order structure.[20] The reported amino acid contents vary, but it could be summarized that in feather keratin, amino acids such as the hydroxyl group containing polar serine (Ser), non-polar and cyclic proline (Pro), non-polar glycine (Gly), acidic asparagine (Asp) and glutamine (Glu), basic arginine (Arg), and non-polar valine (Val) and leucine (Leu) are present to some extent.[18,21,22] Compared to other proteins, keratin also has a relatively high concentration of sulphur-containing cysteine (Cys).[8] Cys residues can form disulfide inter- and intramolecular cross-linking within keratin.[8,23] These disulfide bonds play a major role in determining the physical properties of keratin.[14] In addition to disulfide bonds, amino acid residues present in keratin enable hydrogen bonding, hydrophobic interactions as well as ionic bonds (Figure 6), which again affects the chemical and physical properties of feather keratin.[8,24–26]
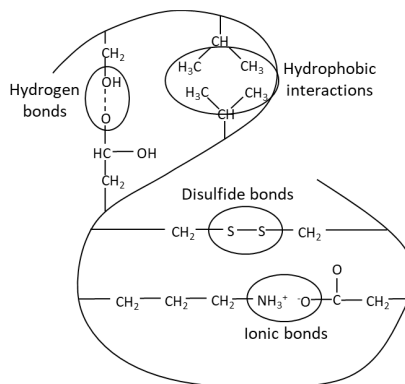
Figure 6. Schematic presentation showing the possible intermolecular and intramolecular bonding of feather keratin (redrawn from Shavandi et al.[8]).

2.1.2 Defining keratin building blocks

Building blocks can be defined as structural components that can be further used to produce intermediates or end products. Building blocks derived from biomass are considered an alternative to fossil-based building blocks in material applications striving toward a sustainable future. The preparation of building blocks from biomass usually requires the deconstruction of the biomass source into its structural components. For example, cellulosic building blocks derived from wood are pulp fibres, cellulose nanofibres, polymeric cellulose and glucose. By understanding the feather keratin structure, feathers could be deconstructed into the following structural components: roughly disintegrated keratin fibres and particles (from a honeycomb structure), finely disintegrated fibrils, extracted keratin polypeptides, oligopeptides and amino acids (Figure 7).

Figure 7. Deconstructing keratin building blocks from feathers. Top row: from complex and hierarchical feather structure into fibrous and powdery form. Bottom row: microscopy image of roughly disintegrated feathers, finely disintegrated feathers and soluble molecular keratin in water.

Feather keratin has a wide range of possible applications that are strongly determined by its structure and properties. The chemical structure of keratin could allow its use in designed forms like micro and nanoparticles, composites, thermoplastics, films, fibres and filaments, hydrogels and sponges, while its natural

properties could make them suitable for feed, fertilizers, flame retardants, absorbents as well as biomedical, cosmetic and electronic applications.[5,27] Keratin has shown potential in wound healing[28], tissue engineering[29], controlled drug release[23], flame retardancy[30,31], skin hydration and elasticity improvment[32], electronic materials[33] and as a bioadsorbent for dye[34], metal ions[35] and oil[36].

Roughly, keratin building blocks derived from feathers can be divided into two categories: **fibrous keratin building blocks** (including different-sized fibres, fibrils and particles) and **molecular keratin building blocks** (including polypeptides, oligopeptides and amino acids). Figure 8 visualizes the difference between the morphologies and macroscale structure of the fibrous and molecular keratin building blocks when used in films. While fibrous keratin has a clear macroscale structure, molecular keratin does not.
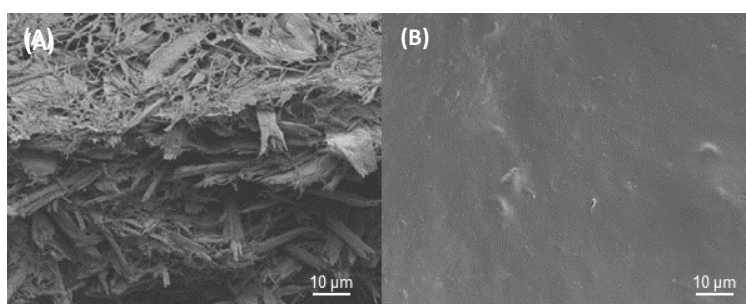
Figure 8. Scanning electron microscopy (SEM) images showing the macroscale structure of films prepared from (a) fibrous and (b) molecular keratin building blocks. Pictures from publications II & IV.

2.2 Preparation of keratin building blocks

The unique structure and properties of feathers, combined with their low cost and wide availability, make them an attractive choice to be used as building blocks for future materials. However, the feather structure as such is rarely applicable, and processing is required to deconstruct feathers into a suitable form for applications. The structure of feathers is stable and resistant due to the extensive disulfide cross-linking, high content of hydrophobic residues and tight packing of α-helices and β-sheets in polypeptide chains.[25,37] Thus, feasible and sustainable processing methods to deconstruct feathers into keratin need to be developed to enable their use. Efforts to process feathers have been carried out, and in this chapter, the most prominent of them will be shortly introduced and discussed. Roughly, the feather processing methods can be categorized into three categories: physical, chemical and biological routes. Feathers should be sanitized before any processing or use. The methods described in this chapter are performed after sanitation.

2.2.1 Physical routes

Physical routes to prepare keratin include treatments like heating, grinding and pressure.[38] Grinding is a mechanical treatment in which mechanical force is applied to crush, cut and break the raw material into smaller particles. Me-

chanical treatments are divided into the following levels depending on the particle sizes aimed: coarse grinding (from cm to mm), intermediate micronization (cm to 100 μm), fine grinding (<100 μm), ultrafine grinding (<30 μm) and nanogrinding (<1 nm).[39,40] Thus, mechanical treatments allow the preparation of various sizes of building blocks quite well. Ground fibrous keratin has been used, for example, in composites together with synthetic polymers[41–44], in extrusion[6] and in thermally processed films[45]. For feathers, mechanical treatments could provide a simple processing method when a small particle size or uniform shape is not required.[46] Furthermore, mechanical treatments are a good choice for pretreatment before other processing methods to enhance their performance, as it makes the raw material more accessible by improving the mass and heat transfer, thus reducing the energy input.[40] Other physical routes that could allow the preparation of keratin building blocks are steam explosion[25,47,48] and pyrolysis[49,50]. These treatments are also simple and efficient and could be considered especially when residual colour, extensive keratin degradation or even a rubbery structure is not a problem for the application. In general, all physical routes have high energy consumption.

2.2.2   Chemical routes

Chemical routes to prepare keratin building blocks include the use of chemical agents such as solvents.[38] They are probably the most studied processing methods for feathers because they allow the preparation of molecular keratin. Molecular keratin has more versatile applicability than the keratin produced by mechanical means. Keratin is insoluble in water and common solvents, especially due to disulfide bonds within the structure of the keratin.[51] Therefore, feather dissolution generally involves the step of cleaving these disulfide bonds by reduction or oxidation.[8] Although these reactions can ensure good yield and undegraded keratin, they usually require chemicals that have poor recyclability, high production costs, and toxicity.[37] Keratin could also be extracted by dissolving it in alkali, but this requires harsh conditions and causes extensive degradation of keratin.[47]

Green solvents including N-methylmorpholine N-oxide (NMMO), ionic liquids (ILs) and deep eutectic solvents (DES) have been of interest in biomass processing. NMMO is a commercial and recyclable solvent used in the Lyocell process.[52] It has also been used to dissolve feathers.[21] Although feathers were completely dissolved in NMMO, only a small part of keratin could be regenerated, and most of it remained in the filtrate as small peptides and amino acids. NMMO appeared to be able to destroy disulfide bonds as well as peptide bonds.[21] Although NMMO can function as a direct solvent for biomass, the process has some drawbacks, such as side reactions and by-product formation that may cause unwanted effects such as biomass and solvent degradation, discolouration of the fibres, weakened performance of the product, increased consumption of stabilizers or thermal runaway reactions.[53]

To overcome the drawbacks of NMMO, ILs have gained interest in biomass processing.[54] As an example, Ioncell-F is a technology in which regenerated cellulose fibres are produced using a superbase-based IL.[55] ILs are defined as salts that are liquid at room temperature. They usually consist of organic cations such

as quaternized aromatic or aliphatic ammonium ions and organic or inorganic anions that are usually either halide anions or anions in which the charge is distributed over several atoms.[54] Thus, ILs involve large ions with conformational flexibility, enabling the liquid state due to small lattice enthalpy and large entropy changes. ILs are chemically and thermally stable, nonflammable and a have low pressure.[56] ILs have been used to dissolve feathers to obtain regenerated keratin.[57–61] In general, after IL treatment, the yield of regenerated keratin has been reported to be rather low (25–88%), and the obtained keratin has lost part of its molecular weight, secondary structure and crystallinity.[37,57–59] Other drawbacks with ILs are processing difficulties related to high viscosity and solvent recycling.[52]

DESs are a newer type of solvent used in biomass processing; they were first presented by Abbot et al.[62] Unlike ILs, DESs consist of solid components that together form a mixture with a melting point lower than its individual components. DES is obtained when the components are mixed in the specific molar ratio in which the system reaches its lowest melting point (Figure 9a), but mixing with other molar ratios may also produce mixtures with lower melting temperatures.[63] The drop in the melting point is due to the hydrogen bonding between the components, which delocalizes the charge and decreases the lattice enthalpy of the system.[62] The most common DESs are formed between choline chloride and carboxylic acids, and there the decrease in the lattice energy is achieved by hydrogen bonding between the halide anion and the amide moiety.[62] However, in general, DESs are systems that are formed from a eutectic mixture of Lewis or Brønsted acids and bases that are capable of associating with each other through hydrogen bonding.[63] For example, carboxylate salt-urea DESs have been introduced.[64] A small addition of water in DES is known to decrease the melting point even further due to a decrease in the lattice energy.[63]

Like ILs, DESs usually have high stability and low vapour pressure and are non-flammable. However, unlike ILs, DESs are commonly relatively easy and inexpensive to prepare and are usually made of non-toxic, biodegradable and biocompatible components.[63] Due to these advantages, they have also gained interest in biomass processing, for example, in cellulose processing with urea-based DESs.[65–67] Choline chloride-urea/oxalic acid DESs have also demonstrated their potential in the extraction of keratin from wool[68–70], while carboxylate salt-urea DESs have shown potential in protein extraction from Brewer's Spent Grain[64]. From the studied carboxylate salt-urea DESs, an aqueous sodium acetate (NaOAc)-urea DES was found to be the most efficient in protein extraction.[64] In NaOAc-urea DES, the hydrogen bonds needed for the melting could be formed between urea (the hydrogen bond donor) and acetate anion (the hydrogen bond acceptor) (Figure 9b). To my knowledge, feather keratin has not been processed with DESs before.
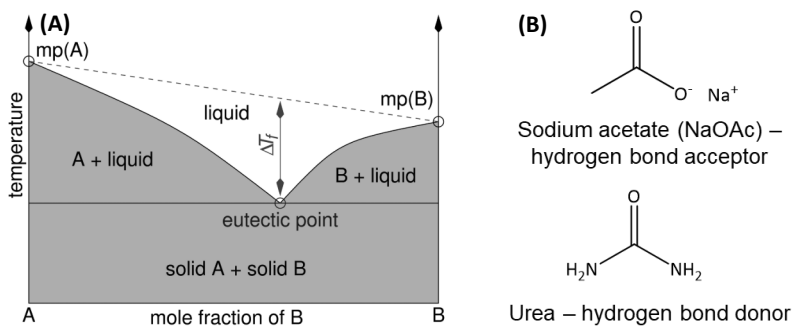
Figure 9. (a) Schematic presentation of how the melting temperature of the mixture changes when two solid components are mixed in different molar ratios. The deep eutectic solvent is formed in the molar ratio in which the eutectic point, the lowest melting point, is reached. (b) Components of sodium acetate-urea DES in which urea acts as the hydrogen bond donor and acetate anion acts as the hydrogen bond acceptor.

2.2.2.1   Dissolution theory

Solubility is determined as the molecular dispersion of a solute in a given solvent in a way that the free energy of the system decreases.[71] Proteins are biological macromolecules or polymers. Hence, their solubility can be described using the Flory-Huggins theory for polymer solubility.[72–74] Flory-Huggins equation describes the free energy change taking place when a non-crystalline polymer is mixed with a solvent, as follows[73]:

$$\frac{\Delta G_m}{RT} = n_1 ln\phi_1 + n_2 ln\phi_2 + \chi\phi_1\phi_2(n_1 + mn_2) \tag{1}$$

where ΔG_m is the free energy of mixing, R is the gas constant, T is the absolute temperature, χ is the Flory interaction parameter, m is the ratio of molar volumes of polymer and solvent, n_1 and n_2 are the number of moles of solvent and polymer, while ϕ_1 and ϕ_2 are the volume fractions of solvent and polymer, respectively.

The Flory interaction parameter is a dimensionless parameter that describes the attraction between the polymer and solvent[72] and depends on the intermolecular forces between the molecules in the system[73]. If ΔG_m is negative, polymer and solvent mix and form a solution spontaneously. The first two terms in Equation 1 describe the entropy of mixing, which is always negative because mixing the polymer and solvent increases the disorder of the system. Thus, to obtain negative free energy, the Flory interaction parameter must either be negative or have a small positive value.[73] The Flory interaction parameter can be determined as follows[72]:

$$\chi = \frac{z\Delta w}{kT} \tag{2}$$

where k is the Boltzmann constant, z is the lattice coordinator number and Δw is the increment energy.

The interactions between the protein and the solvent depend on the properties of the solvent and the structure of the protein.[75] For example, the dielectric constant, the chemical potential, the salt concentration, the viscosity and the surface tension of the solvent are factors that influence the solubility of the protein.[75] On the other hand, the polarity and hydrophobicity, the charge and the molecular weight of the protein affect its solubility.[71]

Protein solubilization will not happen if protein-protein interactions are more favourable than protein-solvent interactions. Some factors decreasing protein solubility are electrostatic attraction between positively and negatively charged moieties, the presence of hydrophobic interactions and a high degree of cross-linking.[76]

Due to the complexity of the feather keratin chemical structure as well as DESs as solvents, dissolution of keratin in DESs is not yet well understood. However, when wool was dissolved in ChCl-urea DES, it was suggested that highly polar Cl^- anion and urea played an important role in disturbing the intra-molecular hydrogen, disulfide and electrostatic bonds in keratin, allowing the dissolution.[68] Urea is well-established as a protein solvent with the ability to unfold proteins.[77]

2.2.3 Biological routes

Biological routes utilize proteolytic enzymes to deconstruct the material[38], and they have also been applied to feathers[78,79]. However, considering the preparation of keratin building blocks for material applications, this route does not appear to be feasible in the near future. The feasibility is limited by the high cost of enzymes.

2.3 Chemical composition and structure of keratin building blocks

The utilization of keratin requires an understanding of its chemical composition and structure. Additionally, the realization of changes during and after processing is critical to ensure optimized preparation methods of keratin for certain applications. The insoluble nature of feather keratin complicates its characterization and decreases the suitability of traditional protein analysis methods. This chapter will introduce different characterization methods that have been applied to study the chemical composition and structure of keratin. The focus will be on methods that reveal information on the characteristics considered determinative in the use of keratin in material applications. Table 1 summarizes the chapter and introduces a toolbox for the characterization of the chemical composition and structure of keratin.

Table 1. Methods to characterize the chemical composition and structure of keratin chosen from the literature.

		Toolbox for Characterization of Keratin Building Blocks		
	Methods	The Principle in Brief	What does it reveal?	Used for feather keratin?
Chemical Composition	Amino acid analysis	Acid hydrolysis & chromatographic separation	Amino acid content (mg/g)	18,21–23,26,78,80,81
	Elemental analysis	Total combustion of the sample and separation of these combustion products by a chromatographic column	Percentages of elements C, H, N, S (%)	12,23,60
	Direct colourimetric method	Determining the concentration of soluble chromophore that has formed from reaction with thiol groups	SH & S-S content (nmol/mg)	25,48
	Size exclusion chromatography (SEC)	Column sorts the molecules according to their size	Molecular weight distribution	21,47,82
	Matrix-assisted laser ionization time-of-flight mass spectrometry (MALDI-TOF MS)	Separation of molecules according to mass-to-charge ratio	Mass-to-charge ratios (m/z) based on molecular weights of the molecules in the sample	23
	Fourier transform infrared spectroscopy (FTIR)	Detection of the intensity of light absorbed by molecular vibrations	Structural fingerprint. Can be used to identify different molecules; percentage of different secondary structures from deconvolution of bands assigned for peptide bonds (-CHNO-)	21,25,48,59
Chemical structure	Nuclear magnetic resonance spectroscopy (NMR)	Detection of the interaction of nuclear spins when placed in a powerful magnetic field	Molecular structure; percentage of different secondary structures from deconvolution of ^{13}C chemical shift of carbonyl	37
	Circular dichroism (CD)	Detection of the difference in absorbance of right- and left-circularly polarized light by the sample	Organized structures of the protein, such as the α-helix or β-fold, give characteristic CD spectra	23
	X-ray diffraction analysis (XRD)	Detection of diffracted beams, which is affected by the spacing of the atoms in the molecule	Crystallinity	25,37,79,83,84

2.3.1 Chemical composition

The amino acid composition and sequence define the interactions and properties of a protein. The amino acid content of feather keratin was already studied in 1964[85], while the sequence was revealed in 1983[18]. The amino acid composition of keratin building blocks is especially valuable when considering their interactions with water or other materials. The amino acid composition can also be used to predict the folding of a protein. In general, the determination of amino acid composition includes the acid hydrolysis of polypeptide chains to obtain its amino acid components, which are then separated with a chromatographic technique. Although there are some differences in the amino acid compositions of keratin, depending on the extraction method or feather source, rather similar amino acid residues have been reported to appear in high concentrations, including Ser, Pro, Gly, Asp, Glu, Arg, Val and Leu.[18,21–23,26,78,80,81]

It is well known that disulfide bonds play an important role in determining the properties of feather keratin.[14] In keratin, sulphur is located mainly in cystine disulfide bonds (-S-S-) and cysteine-free thiol groups (-SH).[51] Amino acid analysis could be used to analyse the content of cysteine residues. But probably the simplest method to determine the sulphur content is elemental analysis in which a sample is first combusted into simpler compounds, which are then detected, giving percentages of carbon, hydrogen, nitrogen and sulfur. The elemental composition has been determined for different structural components of feathers[12] and has been used to complement the results obtained from amino acid analysis[23]. In addition to sulphur content, elemental analysis can be used to determine nitrogen content, which in turn can be used to determine keratin content in composite materials.[60]

Considering the properties of keratin, the separation of -S-S- and -SH contents is valuable because disulfide bonds play such an important role in keratin properties. This kind of determination is difficult for insoluble feather keratin. However, a method has been developed to measure thiol and disulfide levels in hydrophobic and insoluble cereal proteins.[86] The method is a direct colourimetric method in which the sample is suspended in urea to enable a reaction with a colour agent to release a soluble chromophore whose concentration can be determined.[86] This method has been applied for feather keratin to show the decrease in disulfide bonds when the pressure used in the steam explosion was gradually increased.[25,48]

2.3.2 Chemical structure

2.3.2.1 Molecular weight

In material design, the molecular weight of the building blocks plays an important role, especially in the physical properties of the end product. The molecular weight of feather keratin has been reported to be 10 kDa when extracted with urea, phosphate and a reducing agent and measured using osmotic pressure, turbidity, sedimentation rate, and viscosity techniques.[87] Size exclusion chromatography (SEC) and matrix-assisted laser ionization time-of-flight mass spectrometry (MALDI-TOF MS) are common techniques to determine the size or molecular weight of polymers.[88] While SEC uses a column to sort the molecules according to size, in MALDI-TOF MS, ionized molecules are separated according to their mass-to-charge ratio (m/z). The SEC measures the hydrodynamic volume, which is converted to standard molecular weight, while the MALDI-TOF MS measures the mass directly.

When the molecular weight is determined, it is important to realize that it is almost impossible to have a batch of polymers with the exact same molecular weight, and the molecular weight variations are related to the synthesis or fractionation method.[74] Thus, it is important to determine the molecular weight distribution and its polydispersity, which describe the heterogeneity and broadness of the distribution. The SEC gives the number and weight average molecular weights, which can be defined as follows[74]:

$$M_n = \frac{\sum N_i M_i}{\sum N_i} \tag{3}$$

$$M_w = \frac{\sum w_i M_i}{\sum w_i} = \frac{\sum N_i M_i^2}{\sum N_i M_i} \tag{4}$$

where M_n is the number-average molecular weight, M_w is the weight-average molecular weight, N_i is the number of molecules with molecular weight M_i and w_i is the weighting factor for each molecular weight species. The polydispersity index is then determined from the ratio of the weight-average to the number-average molecular weight. The monodisperse sample usually has a ratio of less than 1.1.[74] MALDI-TOF MS does not provide a separate value for the polydispersity, but its resolution and mass accuracy are known to be excellent.[88] MALDI-TOF MS allows molecular ion spectra for individual m/z values, which are based on the molecular weights of the molecular compounds.[89]

Both of these methods have been used to determine the molecular weight of feather keratin. The molecular weight distributions of NMMO treated and steam-exploded feather keratin were analysed with SEC. The distributions were not uniform in their molecular weights, and everything from small peptides to keratin polymers with Mw of 30 kDa was detected.[21,47,82] It was noticed that the buffer that was used to dilute and elute the extracted keratin affected the results.[47] MALDI-TOF MS has been performed to analyse the molecular weight of feather keratin that was extracted using ethanol and hydrochloric acid pretreatments and 2-mercaptoethanol deoxidization. A rather uniform molecular weight distribution of 20 kDa was reported.[23] The results reported indicate that

the molecular weight of keratin remains unclear, but there are methods available that can give indicative information.

2.3.2.2 Conformation of keratin chains

Proteins fold in unique shapes depending on their amino acid content and their order in the primary chain. Keratin is a structural protein, and its structure is dominated by repetitive amino acid sequences that fold to form ordered secondary structures responsible for their properties.[90] Thus, considering material applications, characterization of secondary structures is important. Another interesting aspect is the crystallinity. The organization of the chains is considered to have a role in the physical, chemical, optical and thermal properties of keratin.[12] It is suggested that feather keratin is a semi-crystalline structure[91] that includes crystalline areas with organized and tightly packed molecular chains and amorphous areas with randomly orientated chains.

Spectroscopic techniques can be applied to characterize the secondary structures of keratin. This type of characterization usually means the qualitative identification of α-helices, β-sheets, β-turns and random coils present in the keratin structure. From spectroscopic techniques, Fourier transform infrared (FTIR), nuclear magnetic resonance (NMR) and circular dichroism (CD) spectroscopies are common techniques for analysing the secondary structures of feather keratin.

FTIR spectroscopy is based on molecular vibrations as molecules in the specific bonds absorb infrared light characteristically based on their structure and chemical environment. The spectra are presented in the form of intensity of absorbed light versus wavenumber. The interpretation of the secondary structures is based on the vibrations of peptide bonds (-CHNO-), which have been suggested as being more dependent on the secondary structures of the amino acid backbone than the side chains.[92] Interpretation of different individual secondary structures in feather keratin can be then done using deconvolution techniques.[93,94] Attenuated total reflectance Fourier transform infrared spectroscopy (ATR-FTIR) is an especially recommend technique for different types of solid keratin building blocks because no pre-treatment of the sample is required as it is based on total internal reflection, which is enabled using a crystal that is in close contact with the sample. Keratin gives a characteristic and identifiable FTIR spectrum that can also be used to interpret the changes taking place in the secondary structure of feather keratin after processing.[21,25,48,59] The results obtained from the deconvolution show that feather keratin includes β-sheets, α-helices, turns and random coils, but in different studies, the percentages of different secondary structures vary.[21,25,48,59] Deconvolution data should always be treated with caution as deconvolution of spectroscopic spectra is affected by a variety of parameters, some of which are selected individually. However, all of the studies show that after the feathers are processed, the ordered secondary structures are reduced.[21,25,48,59] Thus, FTIR could be especially useful to determine how the chemical structure of feathers changes during processing.

NMR is a technique based on the study of the energy levels of specific atomic nuclei when the sample is placed in a strong magnetic field and excited by radio waves. Certain nuclei resonate at a characteristic frequency when placed in a

magnetic field, and variations in that resonant frequency reveal detailed information about the chemical environment and thus the molecular structure of the sample. The NMR spectra are based on the magnetic resonance of the nuclei, most commonly ^{13}C and ^{1}H, and it is plotted as signal intensity as a function of chemical shift. In NMR, the samples are usually dissolved, and NMR is carried out in the liquid state, but it can also be performed for solid samples. However, in the solid state, stronger interactions are present, and there is less motion of the molecules, meaning that the measurement takes a longer time and broader peaks are observed. Keratin has a characteristic NMR spectrum and has also been used to interpret secondary structures of keratin.[37] For example, the ^{13}C chemical shift of carbonyl gives a slightly different value depending on whether it is in α-helix or β-sheet structure.[95] The deconvolution of the carbonyl peak of feather keratin showed that random coil and β-sheet conformations dominated over α-helix, and after dissolution in IL, the regenerated keratin had a rather similar structure.[37] Again, the deconvoluted data should be interpreted with caution.

CD spectroscopy measures the difference in absorbance and reflection between right-handed and left-handed circularly polarized light when the light hits asymmetric molecules such as amino acids in proteins. When light adsorbs and refracts, the amplitude decreases and the light wave rotates, leading to elliptically polarized light, which can be expressed as the degree of ellipticity as a function of wavelength. The organized structures of a protein, such as the α-helix or β-fold, give characteristic CD spectra. Common CD spectroscopy requires samples in a liquid state, which makes its use with feather keratin difficult because dissolution of keratin will most probably cause changes in the organized structures of the native insoluble keratin. However, CD has been applied to solubilized feather keratin, and it is suggested that feathers are rich in β-sheets, but after extraction, the structure is changing towards a random coil.[23]

X-ray diffraction analysis (XRD) is a scattering technique usually used to identify the crystalline structure of samples. XRD is based on X-ray beams focused on the sample. The interaction of incident X-ray beams with the sample creates secondary diffracted X-ray beams that are related to the interplanar spacing in the crystalline structure of the sample. When the diffraction angle and intensity of the diffracted beams are detected, a specific diffraction pattern is formed. XRD is a common and suitable technique for studying the crystallinity of feather keratin in different structures such as powders, films and fibres.[91] However, studies on the crystallinity of cellulose have shown that XRD studies in semi-crystalline samples may not be that straightforward.[96–98] Therefore, XRD studies on keratin should also be treated with caution.

In keratin, crystallinity and ordered secondary structures could be related because α-helices and β-sheets can be considered high-order crystalline structures. Thus, diffraction patterns obtained from XRD have also been used to study α-helices and β-sheets structures in feather keratin together with crystallinity.[25,37,79,83,84] It can be concluded that feather keratin has a characteristic diffraction pattern with two clear peaks indicating two different crystalline struc-

tures which could be assigned for α-helices and β-sheets. However, the interpretations considering the degree of crystallinity and the relationship between the crystallinity and ordered secondary structures are not consistent due to overlapping signals.[25,37,79,83,84]

2.4 Self-standing film approach to study keratin building blocks

Preparation of self-standing films is a simple and common way to study the physical properties of materials because they are very suitable for many characterization techniques. The studied physical properties can be then used to complement the structural characterization, allowing an understanding of the suitability of keratin building blocks in different applications. This chapter will describe how self-standing films can be used to study keratin building blocks.

2.4.1 Film formation

To prepare keratin films from feathers, the feathers must be converted into a form that enables the preparation of self-standing films. Suitable processing technologies for feathers were discussed in Section 2.2. After different processing methods, including mechanical and chemical routes, solvent casting is a common and recommended method for preparing films from feather keratin.[5] Solvent casting is a gentle method to prepare films and is therefore not expected to induce additional damage to the structure of the keratin. It is a simple method that can be applied to both fibrous and molecular keratin building blocks. To ensure good quality of the films and, in particular, reproducibility between different samples, there are a few things to consider when preparing the films. The suspension from which the film is cast should be stable with known solid content to form a homogeneous film. The casting support should prevent the film from shrinking during drying and allow the film to be easily removed from it. Self-standing feather keratin films could also be prepared by compression moulding, but heat and pressure can cause changes in the keratin structure.[99,100]

2.4.2 Strategies to improve physical performance

Without any chemical modifications or additives such as plasticizers or cross-linkers, keratin films are fragile.[23,91,101,102] When feathers are processed, keratin partly loses its disulfide bonds, crystallinity, ordered secondary structures and molecular weight, which leads to films with poor mechanical properties and stability.[51,103] Common strategies to improve the film properties include plasticizers and cross-linkers as additives in keratin suspension before casting. Also, chemical modifications like acetylation[99] or carboxymethylation[51,104] of feather keratin or the incorporation of reinforcing nanoparticles into the film structure[103] can be done, but these techniques are not covered in this work.

Plasticizers are usually small molecules that are able to incorporate and position themselves into a protein network and disturb the protein-protein interactions. The plasticizing effect is then gained through increased chain mobility and free volume. Therefore, water also has a plasticizing effect.[105] Feather keratin films have been commonly plasticized with polyols, including glyc-

erol[23,80,91,106], sorbitol[107], and polyethylene glycol (PEG)[108,109]. Plasticizers are essential to prepare films from keratin, and they especially improve the elongation at break. But on the other hand, they usually make the films more hydrophilic, which is a drawback in most of the material applications.

While plasticizers are added to disturb the protein-protein interactions, cross-linkers are added to the protein network to introduce new covalent bonds to the keratin structure, making chain packing tighter and reducing chain mobility. Cross-linking improves the mechanical and barrier properties of protein films.[105] Cross-linking feather keratin has not been extensively studied so far, but protein films could be chemically cross-linked using aldehydes[110,111] or di-epoxies[112]. It is reported that cross-linking keratin with formaldehyde and glutaraldehyde especially improved the wet tensile strength of the films[103], while by cross-linking wool keratin films with diepoxies, the waterproof characteristics were improved and the mechanical properties remained the same[112].

2.4.3 Film characterization

To gain a general understanding of the suitability of keratin building blocks in material applications, the effect of building block preparation methods and added additives on the physical properties of self-standing keratin films should be studied. Table 2 provides a toolbox for characterization of these kinds of films. Methods have been chosen from the literature in a way that they allow a comprehensive understanding of the durability and stability of the films.

Table 2. Methods to characterize keratin films chosen from the literature.

Toolbox for characterization of self-standing keratin films			
	Methods	**What does it reveal?**	**Used for feather keratin**
Film-forming capacity	Visual appearance	Quickly shows if any capacity for film forming exists	
	Scanning electron microscopy (SEM)	Morphology	80,91,102,106–108
Mechanical properties	Mechanical testing	Tensile strength, elongation, deformability and elastic modulus of films	80,91,103,106,107
Interactions with moisture & water	Water vapour permeability (WVP)	Permeability of water vapour in the film structure, interactions of the keratin network with water vapour (moisture)	80,107,108
	Static water contact angle (WCA)	Wettability of keratin film surface, interactions of keratin film surface with water	57,83
	Gravimetric determination of solubility	Percentage of the film that dissolves in water, interactions of keratin film with water	113–115*
	Gravimetric determination of swelling	Moisture uptake, interactions of the keratin film with water vapour (moisture)	113–115*

*Other protein films

2.4.3.1 Evaluation of film-forming capacity

A rough estimation of the film formation capacity can be carried out by assessing the visual appearance. If a nonuniform film is formed or there are clear cracks, there is no film-forming capacity. In general, extracted keratin forms fragile films, and additives are needed to form films that do not crack. However, if a seemingly uniform film is formed, microscopic techniques can be used to characterize the morphology of the films.

Scanning electron microscopy (SEM) is a very common and informative technique for visualizing the topography of films. In SEM, the image is formed when a focused electron beam is scanned across the specimen. Electrons interact with atoms on the surface of the specimen, and reflected signals are detected. The formed signals are capable of resolving details with magnification up to 1 million times.[116] SEM has widely been used in the characterization of feather keratin in film structures. [80,91,102,106–108] SEM images have revealed that the morphology of the keratin films depends on the feather processing method and added additives. In general, keratin that is obtained via chemical routes enables the formation of uniform films, and additives such as glycerol increase the uniformity.

Besides SEM, other techniques like optical microscopy and transmission electron microscopy may also be used to characterize keratin films. But SEM is recommended because of its high magnification, nondestructive evaluation and simple sample preparation.

2.4.3.2 Mechanical properties

Measuring mechanical performance, including tensile strength, strain at break, deformability and elastic modulus of keratin films, is a simple method to evaluate and compare the effect of different building blocks and added additives on film properties. Besides evaluating the suitability of keratin films for some specific applications, the mechanical properties give an insight into the interactions within the film. The mechanical properties of protein films depend on both their composition and environmental conditions.[105] For example, the addition of plasticizers increases the strain at break and decreases the tensile strength by increasing the free volume in the films, while cross-linkers usually increase the tensile strength by introducing new cross-links in the films. In high humidity, hydrophilic films usually adsorb moisture, and water molecules act as a plasticizer in the film structure.[105] When mechanical properties are measured, a film sample is placed between two grips that clamp the material, and force is loaded on the material by stretching it. The change in length of the sample is measured. The tensile test is a common method to test the mechanical properties of keratin films.[80,91,103,106,107] It can be concluded that keratin films give values comparable to other protein films, and additives such as plasticizers and cross-linkers are needed to obtain sufficient mechanical properties for film processing.

2.4.3.3 Interactions with moisture and water

Protein films are mostly hydrophilic, which means that moisture and water have an impact on their performance. Therefore, understanding the interactions with moisture and water is essential. Film structures allow the study of water vapour permeability (WVP), solubility, swelling and water contact angle (WCA).

WVP measures how water vapour is transmitted through a material. thus giving insights into the bulk properties of the film. Moisture permeation through the protein film occurs in four steps. First, water vapour is absorbed on the surface of the film. Secondly, water vapour penetrates the film structure followed by the diffusion of water vapour through the structure. The final step is the desorption of water vapour from the other side of the film surface. The partial difference in water vapour pressure between the two film surfaces is the driving force for the penetration process.[117] The WVP value (10^{-10} g/m^2 s Pa) can be calculated using the following equation[117,118]:

$$WVP = \frac{(WVTR \cdot L)}{\Delta p} \qquad (5)$$

where $WVTR$ is the measured water vapour transmission rate (g/(m^2 s)) through the film, L is the mean thickness (m) and Δp is the partial water vapour pressure difference (Pa).

WVP measurement has been used especially to study how plasticizers modify the properties and structure of feather keratin film.[80,107,108] In general, protein films have high WVP but low gas permeability, and keratin is not an exception. The addition of plasticizers to the film structure further increases the WVP values.[80,107,108]

While WVP is used for bulk properties, WCA is used to study the wettability of the film surface and thus the interactions of water with the film surface. In this measurement, a water drop is placed on the film surface, and the angle between the film surface and a tangent drawn on the droplet surface is measured. The following equation can be used to determine the angle[119]:

$$\gamma_{LV} \cdot cos\theta_{eq} = \gamma_{SV} - \gamma_{SL} \qquad (6)$$

where θ_{eq} is the contact angle at the equilibrium, and γ_{LV}, γ_{SV} and γ_{SL} liquid-vapour, solid-vapour and solid-liquid interfacial tensions, respectively.

Equation 6 is accurate for an ideal surface that is smooth, homogenous, rigid, insoluble and non-reactive, and the wetting dynamics of biopolymers are affected by absorption and spreading of the droplet at the solid-liquid interface.[119] The level of hydrophobicity of feather keratin has been interpreted by measuring the contact angle.[57,83] In general, if the angle is below 90 degrees, the surface is considered hydrophilic.

The determination of the solubility of the films can be simply carried out with gravimetric determination. Solubility can be determined as a percentage of dry matter solubilized in water. It can be simply carried out by immersing film with a known mass (m_o) in water for a certain time and weight the dried sample (m_1) after immersion in the water. The solubility was then calculated using the following equation:

Solubility (%) = 100 x ($m_o - m_1$) / m_o $\qquad (7)$

This method gives information about whether water can break the interactions within the film and thus disintegrate and dissolve it. Although solubility describes the interactions with water, measuring the swelling of the film can give insights into the film-water vapour interactions. Swelling can be determined as a percentage of moisture content in the films after conditioning them at different relative humidity (RH) levels. The mass of the film changes, depending on the uptake of water vapour in its structure. The water vapour uptake, and thus swelling, can be calculated using the following equation:

$$\text{Swelling (\%)} = 100 \times (m_{RH2} - m_{RH1}) / m_{RH1} \qquad (8)$$

where m_{RH2} is the mass of the film at the higher RH, and m_{RH1} is the mass of the film at the initial RH.

It seems that the measurement of the solubility and swelling of feather keratin films has not been done extensively, but they are techniques used in protein film characterization when the effect of cross-linking has been evaluated.[113–115]

2.5 Thin film approach to studying interactions between keratin and lignocellulosic materials

A deep understanding of the interactions of keratin with other biomaterials like lignocellulosic materials is critical to ensure the optimized development of future keratin-based materials. Some attempts have already been made to combine feather keratin with cellulose[60,120,121] and lignin[122], but the combination of keratin and lignocellulosics is still relatively unexplored, and we are still lacking a fundamental understanding of the interactions between keratin, cellulose and lignin. This kind of nanoscale understanding of interactions between two materials can be obtained by studying the adsorption of keratin onto thin films made of lignocellulosic building blocks. This chapter describes the preparation of the thin films and how keratin adsorption onto them can be studied.

2.5.1 Preparation of cellulose and lignin thin films to study keratin adsorption

Thin films can be considered as model films, allowing the study of complex natural materials with sensitive surface techniques. Probably the most used method to prepare thin films is the spin-coating technique. However, other methods, such as Langmuir-Blodgett (LB) deposition and adsorption, have also been reported.[123]

In the spin-coating process, the polymer-containing liquid is spread onto a rotating substrate, whereafter the liquid is evaporated with the help of high-speed spinning, leaving a uniform polymer film. The thickness and roughness of the thin films can be controlled by altering parameters such as the solution concentration and solvent choice and the acceleration, speed and duration of the spinning.

Spin coating, as a fast and rather simple method, has been shown to enable the preparation of smooth thin films of cellulose.[124,125] The method introduced by Kontturi et al.[124,125] involves first spin-coating hydrophobic and well-soluble

trimethylsilyl cellulose (TMSC) on the substrate, and then the TMSC is hydro-lyzed to cellulose using hydrochloric acid . The method of using TMSC to pre-pare cellulose thin films was first developed for the preparation of LB-films[126,127] and later also used for the faster spin-coating method.

Smooth and fully covered lignin thin films have also been successfully pre-pared with the spin-coating technique.[128] Actually, spin-coating is a good tech-nique to prepare lignin thin films as the poor solubility of lignin limits the use of the LB technique. The procedure is rather simple, as first lignin is dissolved in 1.4-dioxane followed by spin coating on the substrate.[128]

Lignin thin films can also be prepared in other ways. Farooq et al.[129] intro-duced a method to prepare lignin films from colloidal lignin particles (CLP). Compared to dissolved lignin, CLPs have different orientations of functional groups and a spherical nature. Direct adsorption was found to be an optimal method to prepare CLP thin films. In this method, the CLP solution is allowed to adsorb onto the substrate by simply submerging it for a certain time followed by rinsing and drying.[129] Since the properties of the CLP particles are slightly different from those of dissolved lignin, a study using both types of lignin sur-faces could allow for a more comprehensive understanding of the interactions in protein adsorption.

2.5.2 In-situ protein adsorption

Protein adsorption studies on thin films are usually carried out using a flow chamber in which protein solution is passed over the surface. Quartz-crystal mi-crobalance with dissipation monitoring (QCM-D) is a surface-sensitive tech-nique that allows in-situ monitoring of the mass changes taking place at the solid-liquid or solid-gas interfaces. Thus, QCM-D enables the measurement of mass changes due to protein adsorption and desorption as well as water uptake. In addition to mass changes, QCM-D provides information on viscoelastic prop-erties and possible structural changes in the adsorbed layer.

The technique is based on an inverse piezoelectric effect. A quartz sensor os-cillates in an electronic field at its resonance frequency (f_o) and its overtones. The resonance frequency changes when the mass on the sensor changes.[130] For adsorbed layers that are evenly distributed, rigid, fully elastic and have a small mass compared to the sensor itself, the frequency change is proportional to the change in areal mass, as described in the Sauerbrey equation:[131,132]

$$\Delta f = -\Delta m / nC \qquad (9)$$

where $\Delta f = f - f_0$ is the change in frequency (Hz), Δm is the change in mass ($mg \cdot m^{-2}$), C is the mass sensitivity constant ($C = 0.177 mg \cdot m^{-2} \cdot Hz^{-1}$) and n is the overtone number (n=1,3,...).

When the voltage is turned off, the oscillation gradually decreases. The reso-nance amplitude is reduced due to frictional losses at a rate that depends on the viscoelastic properties of the layer attached to the surface of the sensor. Atten-uation amplitude, dissipation (D), can be determined with the following equa-tion:[133]

$$D = \frac{E_{dis}}{2\pi E_{st}} \qquad\qquad (10)$$

where E_{dis} is the dissipated energy and E_{st} is the stored energy during one oscillation cycle; $\Delta D = D - D_0$ is the dissipation change, where D_0 is the dissipation of the sensor in the buffer before the measurement; and D is the dissipation at any given time during the measurement. Dissipation changes reveal insights into the rigidity of the layer, which can be related to the hydration level or the conformation of adsorbed proteins.

For a system in which large dissipation is observed, the Sauerbrey equation is not suitable as it is only valid when the adsorbed layer is rigid. Siow et al.[134] justified the validity of the Sauerbrey equation by recording the frequencies of five overtones and showing that the variations were less than 3 Hz after normalization by the overtone numbers. This indicated rather rigid films. For systems with a large dissipation, a Voigt viscoelastic model is more accurate. In the study by Dutta et al.[135], the differences between the Sauerbrey equation and the Voigt viscoelastic model to calculate the adsorbed mass were nicely demonstrated. It was observed that the masses calculated with the Sauerbrey equation gave lower values than the Voigt model, but the differences were smaller when the layer was considered rigid. When the adsorbed mass is calculated from QCM-D data, the calculated mass includes both adsorbed protein and the bound water in the adsorbed protein layer.

Protein adsorption has been studied on both cellulose[136,137] and lignin thin films[138–140] using QCM-D, but to my knowledge, keratin adsorption has not been previously explored.

2.5.3 Protein adsorption on surfaces made of lignocellulosic materials

When the free energy of an interface between two phases is higher than the free energy of a bulk phase, molecules accumulate at the interfaces to decrease the energy. Hence, the surface of the substrate tends to adsorb any molecule that differs from the solvent molecules to increase its stability.[141,142] However, in solution, simple and uncharged polymers adopt flexible and high entropy structures, which means that their entropy decreases when they adsorb. Thus, in order for them to adsorb on the surface, the entropy gain due to the release of solvent molecules and the free energy of the binding must be more favourable to cover the loss of conformational entropy.[143,144] However, proteins are complex polymers, and their hydrophobicity, charge, size and structural stability affect their adsorption.[145] In general, nonspecific protein adsorption in aqueous environment on solid surfaces is driven by dehydration of the sorbent surface and parts of the protein molecule, electrostatic interactions between the protein and the sorbent, and structural arrangements of the protein.[143] Protein adsorption occurs spontaneously if the Gibbs energy of the system decreases:[142]

$$\Delta_{ads}G = (\Delta_{ads}H - T\Delta_{ads}S) < 0 \qquad\qquad (11)$$

where $\Delta_{ads}H$ is the change in the enthalpy during the adsorption, $\Delta_{ads}S$ is the change in entropy and T is the temperature.

The negative Gibbs energy and thus the spontaneous protein adsorption on the hydrophobic surface are mainly driven by the increase in entropy due to solvent molecule ordering. The gain in entropy is mainly obtained from dehydration of the surface since the bound solvent molecules and counter ions are released into the bulk phase and the loss of the ordered conformation of proteins as they arrange themselves to match the binding sites of the surface.[142] On hydrophilic surfaces, the effect of dehydration is less distinct, and the gain in entropy is obtained mainly from the reduction of the ordered structures of proteins upon adsorption, leading to a higher gain in conformational entropy. Protein flexibility is known to be beneficial for adsorption since they are more sensitive to surface-induced structural changes, allowing the key residues to arrange appropriately in relation to the binding site.[143] This effect has been observed when proteins are adsorbed on lignin surfaces.[138,146]

Besides, the entropy changes, the interactions within the system play a role in the adsorption. Electrostatic interactions can drive adsorption, and it has been observed that negatively charged protein adsorption can increase when the cellulose substrate is cationic.[137,147] However, ensuring the opposite charges does not always guarantee the highest adsorption. Proteins carry a positive net charge when pH is below their isoelectric point (IEP), while above their IEP, they are negatively charged. When the pH of the system is at the IEP of the protein, it has a coiled conformation and the net surface charge is zero, causing poor solubility. The adsorption of a protein at IEP on lignocellulosic surfaces has been found to be higher compared to other pH levels[137,148]. The high adsorption was explained by the better packing capacity of neutral proteins, allowing greater surface coverage.[148] Another explanation could be decreased interactions with the solvent since the layer formed at IEP was observed to be not as hydrated as at other pH levels.[148] In addition to IEP, it is important to understand that the adsorption environment affects the adsorption behaviour. For example, soy protein adsorption on cellulose showed that at higher ionic strength, the adsorbed layer was more compact and rigid compared to the layers adsorbed at low ionic strength. When electrostatic interactions are screened, there is less bound water, and protein chains do not extend out into the surrounding medium but rather lie flat on the surface.[136]

The hydrophilicity of the surface affects the adsorption. Soy protein was adsorbed to a lesser extent on hydrophilic cellulose[136] compared to hydrophobic lignin[140] surfaces. Besides the hydrophobicity, roughness[136,147] and swelling[149] of the substrate have been suggested as affecting the protein adsorption.

3. Experimental

This chapter summarizes the materials and methods used in this work. The preparation of molecular keratin fractions using a DES process is described first. The methods to characterize these fractions are also covered. Secondly, the alkaline pre-treatment followed by the milling of feathers to prepare fibrous keratin is defined. The third section contains information about the self-standing film approach for studying the prepared keratins and the thin film approach for studying the adsorption of keratin on lignocellulosic materials. Detailed descriptions of materials and methods can be found in the materials and methods sections of the original **publications I–IV**.

3.1 Deep eutectic solvent (DES) process to produce molecular keratin

3.1.1 Effect of dissolution time and temperature

Sanitized chicken feathers supplied by Grupo Sada (Madrid, Spain) were ground into 2–15 mm pieces using an E-compactor (VTT, Finland) in which the feathers are pressed through a die using pan grinder rollers. The dissolution of the feathers in the aqueous DES was carried out with the set-up presented in Figure 10 (**Publication I**).

In brief, the aqueous DES and other low melting mixtures were prepared from sodium acetate (NaOAc) or choline chloride (ChCl) and urea by mixing the solid components in the specific molar ratios (1:2, 1:3) with water (10% by weight) in a reaction flask at 80–100 °C under continuous stirring until a clear solution was obtained.

Feathers (2 wt%) were added the the prepared DESs. The total weight of the solution was 150 g. ChCl–urea (90 wt%) in the molar ratio of 1:2 and 8 M urea were used as reference solvents for NaOAc–urea. The solution was mixed from 2 h to 24 h, as indicated later in the text. After the desired dissolution time was reached, the solution was filtered through a metal wire mesh to separate the undissolved particles from the solution. The solid residue was washed with water and freeze-dried to obtain its gravimetric yield. The filtrate was added to 350 ml of water to regenerate and precipitate the dissolved feather keratin and dissolve the DES components. Some of the dissolved keratin remained soluble in water together with diluted DES components. Regenerated keratin was then filtered, washed with water and freeze-dried.
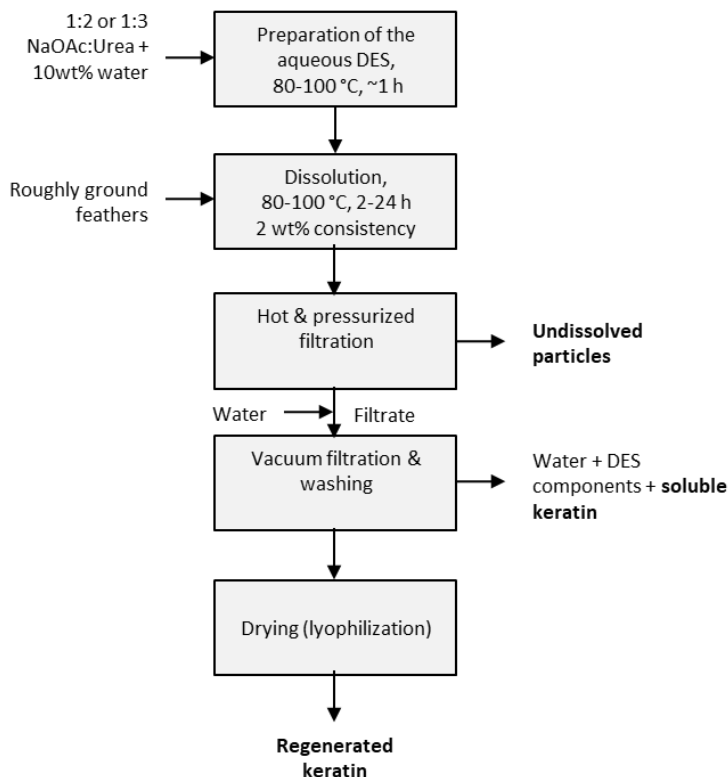
Figure 10. Experimental setup to study the effect of dissolution time and temperature on the DES process to dissolve feathers.

To elucidate the effect of dissolution time and temperature on keratin properties, regenerated keratin samples were extensively characterized using many different methods, summarized in Table 3 (**Publication I**). First, the yields of every fraction (undissolved particles, regenerated keratin and soluble keratin) were determined by gravimetric analysis or using a commercial protein assay kit. The effect of dissolution time and temperature on the chemical composition and structure of regenerated keratin samples was also elucidated. Elemental analysis was carried out to determine the sulphur content, while the direct colourimetric assay was used to determine the SH and S-S content in the samples. MALDI-TOF MS was used to follow the molecular weight of the keratin samples. Secondary structures were studied using ATR-FTIR and NMR. Deconvolution techniques were applied to the spectra to reveal each secondary structure according to studies by Tsuboi et al.[93], Rintoul et al.[94], Duer et al.[95] and Idris et al.[37]. Crystallinity of the samples was studied with XRD, and deconvolution was carried out according to the study of Cao & Billows.[150]

Table 3. Characterization methods applied in this work for the prepared molecular and fibrous keratin fractions and self-standing films.

Characterization methods	Molecular keratin via chemical route						Fibrous keratin via mechanical route		Publication
	Undissolved particles	Regenerated keratin	Soluble keratin	Buffer-soluble keratin	Self-standing films from re-generated keratin	Self-standing films from soluble keratin	Alkaline suspension	Self-standing films	
Yield	x	x	x						I
Elemental analysis		x							I
Direct colourimetric method		x							I
SEC									III
MALDI-TOF MS		x	x						I, II
FTIR		x				x			I, II
NMR		x				x			I, II
CD				x					III
XRD		x							I
Solubility				x					III
Zeta potential				x					III
Optical microscopy					x	x	x	x	II, IV
SEM					x	x		x	II, IV
Tensile testing					x	x		x	II, IV
WPA					x	x			II
Contact angle					x				II
Solubility & swelling					x				II
QCM-D				x					III

3.1.2 Molecular keratin for self-standing film structures and interaction studies

DES-processed keratin was utilized to prepare self-standing film structures and study its adsorption on thin films. The preparation procedure for the DES process follows the procedure introduced in Section 3.1.1 with small modifications (Figure 11, **publications II–III**). NaOAc–urea DES was prepared in the 1:3 molar ratio and with 10 wt% water addition and sanitized chicken feathers (Grupo Sada, Madrid, Spain) were added with 8 wt% consistency. The experiment was carried out on a 15 kg scale. In this procedure, only two fractions were obtained as regenerated keratin was combined with the undissolved particles. The fraction was further dried and ball milled; it was called the high Mw keratin fraction. The soluble keratin fraction was further collected from dialysis. The soluble keratin fraction was freeze-dried and called the low Mw keratin fraction. The Mw distributions of the fractions were determined with MALDI-TOF MS (Table 3, **Publication II**). For the low Mw keratin fraction, CD spectra for the secondary structure and SEC for the molecular weight distribution were also analysed (Table 3, **Publication III**).
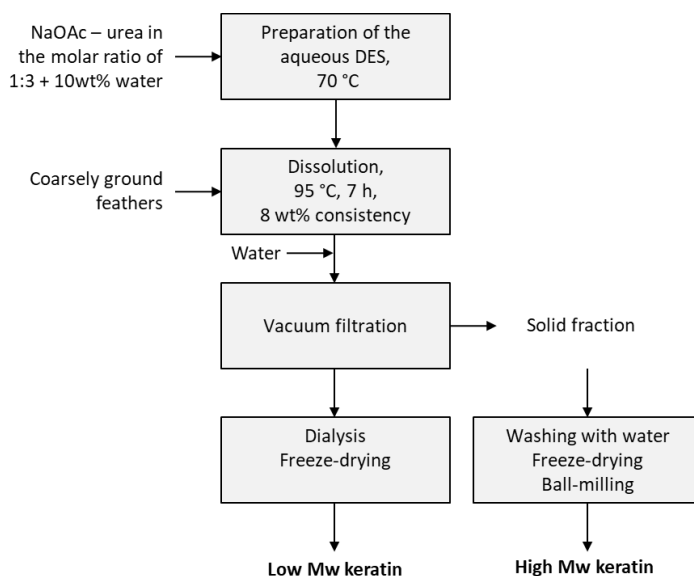
Figure 11. Experimental setup of the DES process to prepare molecular keratin for self-standing film structures and QCM-D adsorption studies.

3.2 Alkaline pre-treatment and milling of feathers to prepare fibrous keratin

The experimental setup for alkaline pretreatment and feather grinding is presented in Figure 12 (**Publication IV**). Sanitized chicken feathers (Grupo Sada, Madrid, Spain) were pre-treated with alkali followed by washing with water and drying in an oven at 105 °C. The milling was carried out using a three-stage mechanical milling process consisting of crushing, grinding, and microfluidization. Pre-treated feathers were compactor crushed into pieces 1-3 cm in length. The

water was then added to form a suspension with 10% consistency. This suspension was then passed six times through a Masuko grinder. Finally, the suspension was passed four times through a microfluidizer.
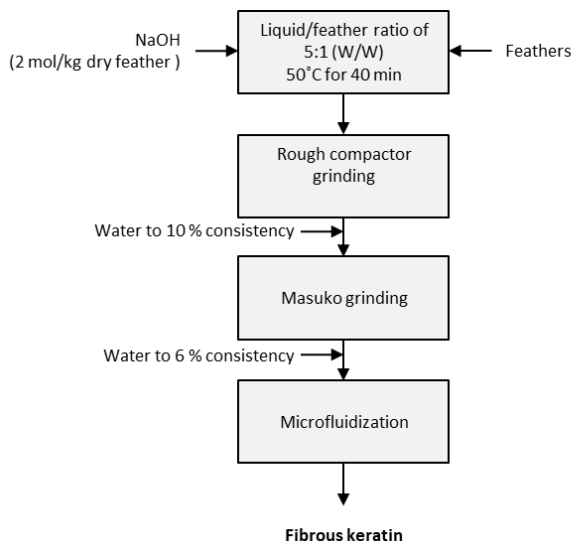
Figure 12. Experimental setup of the alkaline pre-treatment and milling to prepare fibrous keratin for self-standing film structures.

3.3 Solvent-cast keratin films to study the physical properties of keratin

Self-standing films were prepared from molecular (DES-processed) and fibrous (alkaline pre-treated and milled) keratin by the solvent-casting method (Figure 13).
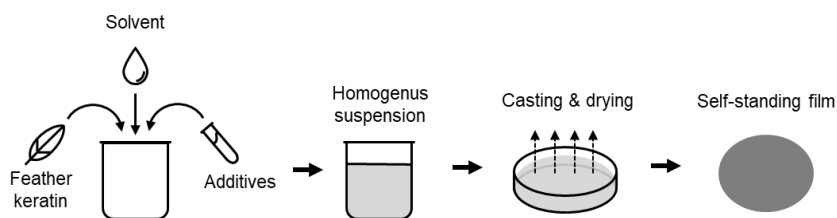
Figure 13. Preparation of solvent-cast keratin films.

The experimental setup to prepare films from high and low molecular keratin fractions obtained from the DES process is presented in Figure 14 (**Publication II**). Figure 14 also shows the preparation of the suspension from which the films were cast. Films were plasticized with glycerol and cross-linked with glutaraldehyde (GA) and 1.4-butanediol diglycidyl ether (BDE). The concentration of glycerol in the film solution was 15 or 30 wt%. The mixtures were cast in silicone or Teflon moulds, depending on the analysis carried out. Cross-linkers, GA and

BDE were added at a concentration of 0.1 g per 1 g of keratin. To ensure an optimal cross-linking effect, GA was added to the mixtures when the pH was adjusted to 9 or 12, while BDE was added when the pH was adjusted to 9.5.
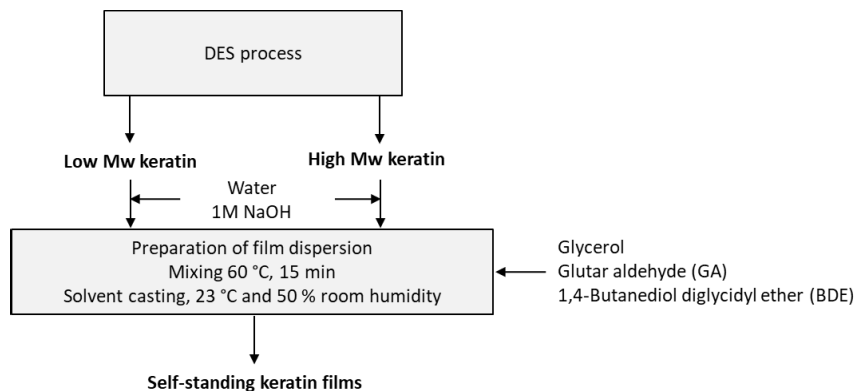
Figure 14. Experimental set-up to prepare self-standing film structures from molecular (low and high Mw) keratin.

The suspensions made of alkaline pre-treated and milled feathers together with additives were cast to prepare self-standing films (Figure 15, **Publication IV**). The effect of various additives on film formation and properties was evaluated. The additives used were 1.4-butanediol, calcium chloride ($CaCl_2$), citric acid, D-sorbitol, ethanolamine, ferric perchlorate ($Fe(ClO_4)_3 \cdot 9\ H_2O$), formamide, glycerol, glyoxal, magnesium chloride hexahydrate ($MgCl_2 \cdot 6\ H_2O$), maleic acid, sodium alginate, sodium hypophosphite monohydrate ($NaPO_2H_2 \cdot H_2O$) and urea. The additives were added at 20−45% by weight.
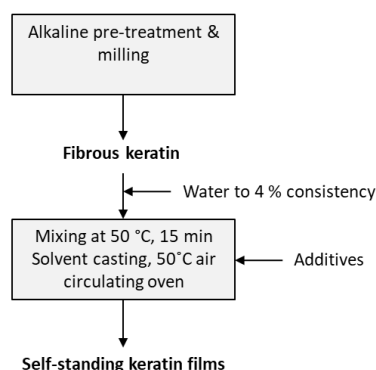
Figure 15. Experimental set-up to prepare self-standing film structures from fibrous keratin.

SEM and tensile testing were used to study the morphology and the mechanical properties of the films prepared from molecular (DES process) and fibrous (alkaline pre-treatment and milling) keratin (Table 3, **Publication II and IV**).

Film structures prepared from molecular keratin also allowed more extensive characterization (Table 3, **Publication II**). Besides SEM imaging, the films

were visualized with optical microscopy. The moisture sensitivity of the film structures was studied using the WVP measurement. The films prepared from high Mw keratin were also tested for their solubility and swelling in water. Furthermore, WCA measurements were carried out to study the wettability of the surfaces. To get insights into the effect of the cross-linkers (GA and BDE) in the chemical structure of the films, ATR-FTIR and NMR spectra were measured.

3.4 Quartz crystal microbalance with dissipation monitoring (QCM-D) to study the interactions of keratin

The in-situ adsorption of DES-processed keratin peptides dissolved in aqueous buffers on the surfaces of thin films of cellulose, lignin and colloidal lignin particles (CLPs) was monitored using a QCM-D device.

3.4.1 Thin film preparation

All the model films were prepared on QCM-D gold sensors (**Publication III**). Cellulose thin films were made of trimethylsilyl cellulose (TMSC) using a spin-coating technique.[125] TMSC-coated sensors were then regenerated to cellulose by simple acid hydrolysis. Two types of lignin films were produced. Lignin thin films of dissolved lignin were prepared using a spin coating technique, while thin films of CLP were prepared using an adsorption method (Figure 16).[129]
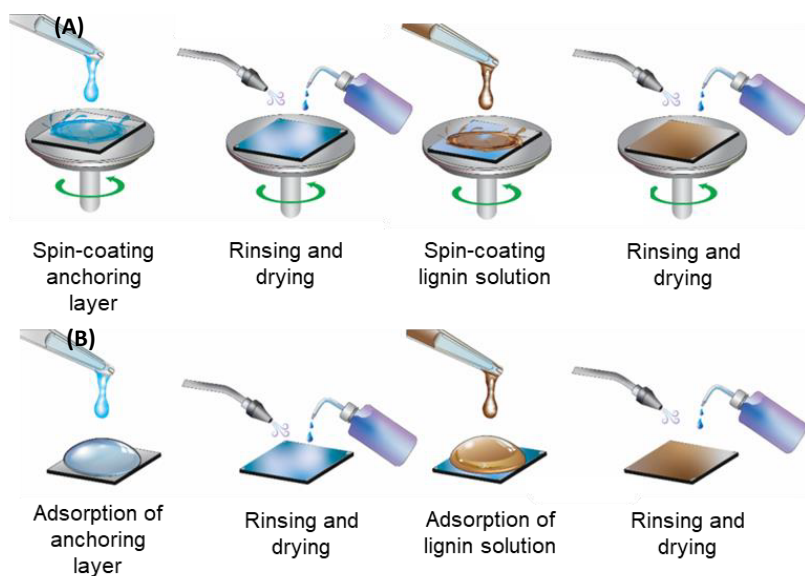
Figure 16. Schematic illustration of the preparation of lignin thin films using (a) spin-coating and (b) adsorption techniques. Adopted from Farooq et al.[129]

3.4.2 In situ adsorption

Keratin solutions for QCM-D experiments were prepared from the low Mw keratin fraction (Figure 11, **Publication III**). To measure the solubility and zeta potential of the low Mw keratin fraction, it was dissolved in water and the pH of the solution was adjusted to 3. 5 and 7 using HCl as well as NaOH. The

insoluble keratin fraction was removed by centrifugation. The amount of soluble protein and its zeta potential were measured from the supernatant.

For the QCM-D experiments, the low Mw keratin fraction was dissolved in several buffers: sodium phosphate buffer (SPB) (pH 7, 50 mM, 150 mM, 500 mM), sodium acetate buffer (SAB) (pH 5, 50 mM) and McIlvaine buffer (pH 3, about 40 mM). Insoluble keratin was separated by centrifugation, and solubility was measured to ensure that all samples had the same concentration (0.1 mg/ml) in the adsorption studies.

Adsorption of keratin on the prepared model films was studied using a QCM-D in continuous flow mode at room temperature. First, the used buffer, in which keratin was dissolved, was injected to stabilize the system. The keratin solution was then pumped with a 0.1 ml/min flow rate for 60 minutes. This was followed by a rinsing step with buffer for approximately 60 minutes to remove reversibly adsorbed keratin

4. Results and discussion

This chapter responds to the aim of the thesis, which was to understand how feathers could be converted into utilizable keratin fractions and to evaluate their potential as building blocks for future materials. To improve the processability of feathers, molecular and fibrous keratin building blocks were generated by the DES process (**publications I–III**) and a simpler milling process (**Publication IV**), respectively. The potential of molecular and fibrous keratin building blocks as self-standing film structures was explored (**publications II & IV**). Finally, to evaluate the opportunity to prepare combined materials, the interactions of keratin peptides with cellulose and lignin were studied (**Publication III**). Figure 16 shows the studied keratin fractions and summarizes the work carried out.
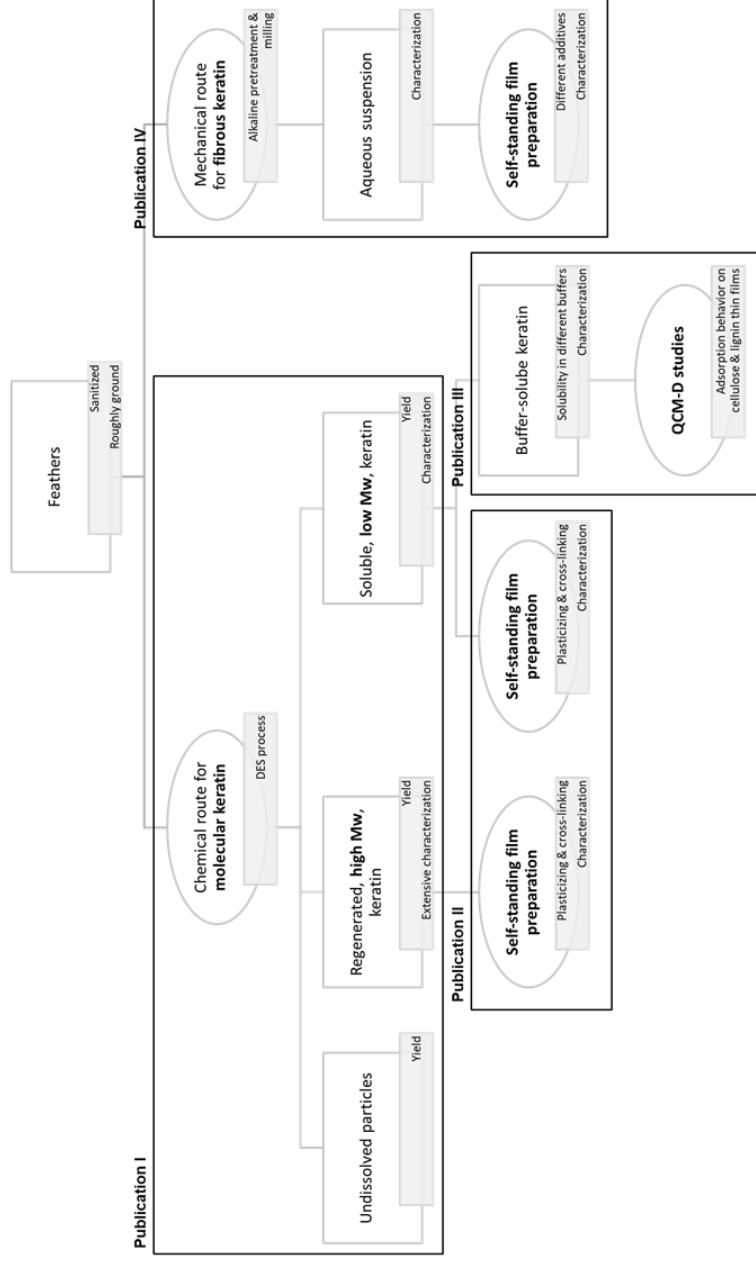
Figure 17. Scheme of the work carried out in the dissertation aiming to explore the potential of feather keratin as a building block for future materials.

4.1 Preparation and characterization of molecular keratin from DES-processed feathers

To enable the versatile utilization of feather keratin as a raw material in material applications, processing is required. An optimal processing method is environmentally friendly, technically and economically feasible and produces keratin in a form suitable for a variety of applications. A scalable DES dissolution as a chemical route was chosen to process the feathers in this study. The DES used was composed of sodium acetate (NaOAc) and urea, which are inexpensive components. While NaOAc is safer for the environment than many other chemicals because it is not chloride-based and is used as a food additive[64], urea can be considered an environmentally friendly chemical because it is already used as a fertilizer.

4.1.1 Effect of time and temperature on the dissolution and regeneration of feather keratin

In **Publication I**, the DES process was first optimized by studying how the treatment time and solvent temperature affected the yields of different keratin fractions (Figure 10). The effects of dissolution time and temperature were also studied by characterizing the chemical composition and structure of the regenerated keratin fraction using the characterization methods shown in Table 3. The used NaOAc-urea DES was compared to 8 M urea and ChCl-urea DES with respect to yields. ChCl-urea can be considered the most recognized DES.[62]

In the used DES process, yields of undissolved feathers, regenerated keratin and soluble keratin were analysed to obtain mass balances. The part that not be identified as one of the three fractions was called the unidentified part. Figure 18 shows the yields obtained for each keratin fraction when the dissolution time and temperature varied from 2 h to 24 h and from 80 °C to 100 °C.

As expected, as the dissolution time and temperature increased, the yield of undissolved particles decreased (Figure 18a,b). When the dissolution time was increased from 2 h to 24 h, the yield of the soluble fraction increased from 10% to 27%, while the unidentified fraction increased from 12% to 38% (Figure 18a). When dissolution time was increased from 2 h to 14 h, the yield of regenerated keratin also increased from 1% to 35% but then started to decrease, reaching the value of 23% after a 24 h dissolution time (Figure 18a). In the beginning, the increase of regenerated keratin, soluble keratin and unidentified fractions occurred concurrently, but after the 14 h dissolution time, the increase of soluble and unidentified fractions started to dominate. It is likely that the keratin polypeptides started to degrade more extensively as the dissolution time increased and that the unidentified fraction was composed of keratin molecules that were too small to be detected with the BCA protein assay kit that was used. The extensive degradation of feather keratin in NMMO dissolution has also been previously observed.[21] When the dissolution temperature was 100 °C and the was 6 h (Figure 18b), 86% of the feathers were dissolved and the highest yield for regenerated keratin (45%) was obtained. At the same time, the unidentified fraction remained rather low, indicating that the increased temperature had a significant effect on dissolution efficiency. This was mainly related to the decreased viscosity of the DES, which improved dissolution by improving the transfer of the DES component to the feather structure.[69,151,152] Also, a small amount of water enhanced dissolution by decreasing the viscosity of the mixture but most

probably did not compete with hydrogen bonding between the DES components and keratin, which is responsible for dissolution.[153] The dissolution yield of 86% is comparable with other previously reported methods. Sharma et al.[154] dissolved feathers in 0.5 M sodium sulfide which can dissolve 80% of feathers, while in the study of Yin et al.[23], feathers were treated with ethanol pre-treatment, hydrochloric acid pretreatment and 2-mercaptoethanol, allowing 90% of the feathers to be dissolved.

For comparison, the dissolution effect of urea (8 M) and ChCl-urea was also measured (Figure 18c). Although ChCl-urea has been reported to be capable of dissolving wool keratin,[68,69] for feather keratin, the dissolution effect was negligible (Figure 18c). 8 M urea was able to dissolve feathers, and the yield of undissolved feathers was even lower than with the NaOAc-urea DES in the molar ratio of 1:2 (Figure 18c). This was partly expected because urea is well-established as a protein solvent. However, with 8 M urea, all dissolved keratin was in soluble form, and precipitated regenerated keratin was not obtained. When the ratio of urea in NaOAc-urea DES was increased from 1:2 to 1:3, its capability to dissolve feathers improved. Thus, the yields of different fractions can be tuned not only with the dissolution conditions but also by tuning the ratio of NaOAc and urea.
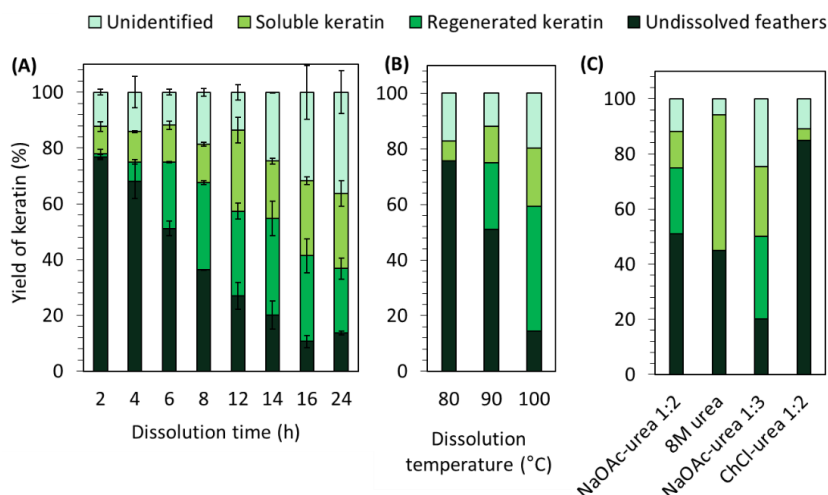
Figure 18. The yields of each keratin fraction when feathers were dissolved in the aqueous DES comprised of NaOAc and urea in the molar ratio of 1:2 (a) at 90 °C for 2–24 h and (b) at 80–100 °C for 6 h. The dissolution was also carried out with 8 M urea, aqueous NaOAc-urea DES with a molar ratio of 1:3 and aqueous ChCl-urea DES in a molar ratio of 1:2 at 90 °C for 6 h. Adapted from Publication I.

The regenerated keratin was characterized by its disulfide and total sulphur contents, molecular weight, secondary structure and crystallinity (Table 3). The results obtained for secondary structures and crystallinity should be treated with caution because they were obtained from the deconvolution of bands in spectra, and the deconvolution of spectroscopic spectra is affected by a variety of parameters, some of which are selected individually. Thus, several characterization methods were carried out to complement each other. Although disulfide bonds, which are largely responsible for keratin stability, decreased (Figure 19d), and even smaller keratin fragments began to form upon increasing both

38

dissolution time and temperature (Figure 19a), ATR-FTIR and NMR showed no major chemical changes in the polypeptide backbone of regenerated keratin (**Publication I**). However, after deconvolution of the bands, it was observed that both the ordered secondary structures (Figure 19b,c) and the crystallinity (Figure 19c) were partly lost. Similar effects have previously been observed when feathers were dissolved in NMMO[21] and ILs[37,59]. Disulfide bonding, ordered secondary structures and crystallinity are believed to be important factors in the strength and stiffness of keratin.[82]
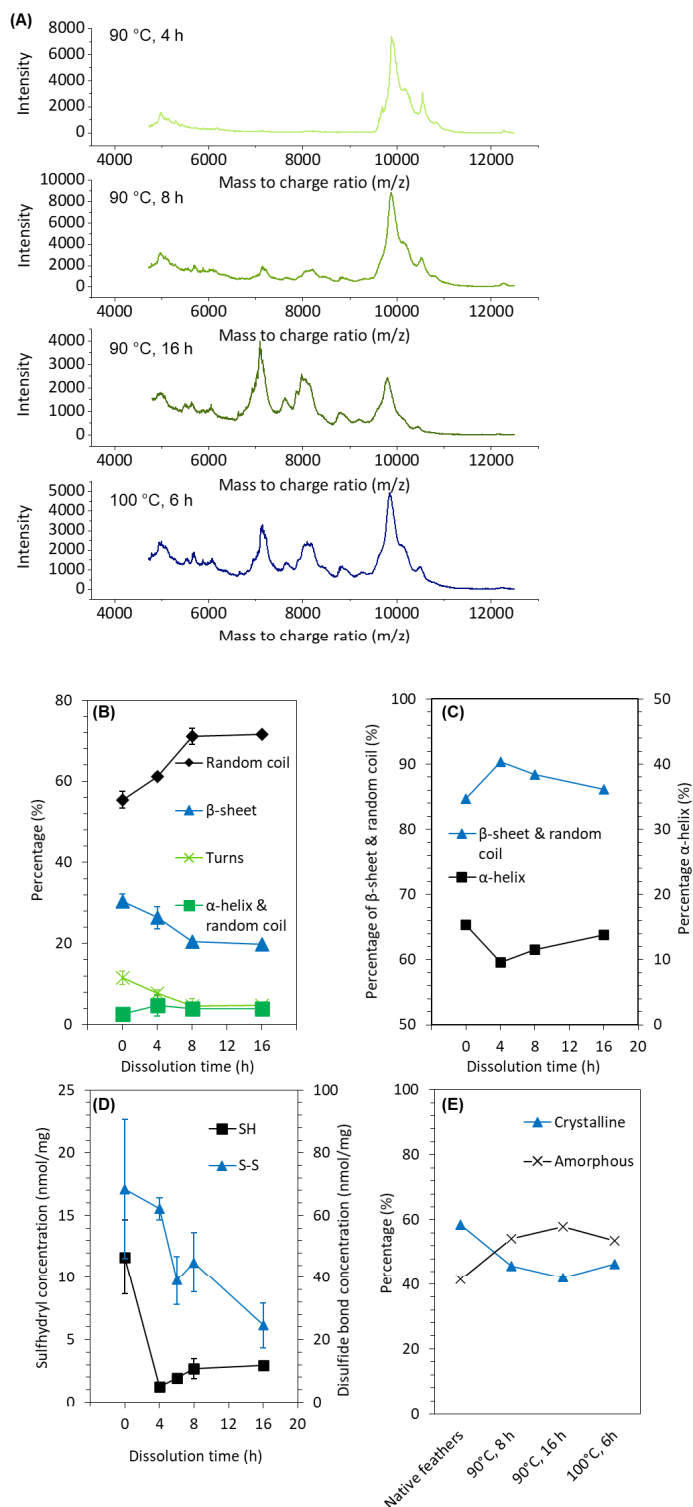
Figure 19. Effect of increased dissolution time and temperature on (A) molecular weight (from MALDI-TOF MS), (B,C) secondary structures (from deconvolution of [B] ATR-FTIR & [C] NMR spectra), (D) S-S and SH contents (from direct colourimetric method) and (E) crystallinity (from XRD) of the regenerated keratin fraction when the feathers were dissolved in aqueous DES. Adapted from Publication I.

The dissolution of keratin and the structural changes of regenerated keratin seem to be due to the ability of the aqueous DES to disturb the interactions within the feather keratin, including cleavage of the disulfide bonds and partly breaking down the polypeptide backbone of keratin. The exact dissolution mechanism is not known, but it can be speculated that the acetate anion, urea and strong interactions between the DES components are important, as explained below.

NaOAc-urea dissolved the feathers better than ChCl-urea (Figure 18c). Acetate anion is known to have higher basicity than chloride[155], which could explain the better solubilization in NaOAc-urea compared to ChCl-urea. Urea is known to unfold protein structures.[77] Although NaOAc-urea DES showed efficient solvation capacity for feathers, regenerated keratin retained part of its ordered secondary structures and crystallinity (Figure 19). In some cases, DESs can stabilize the secondary structure of proteins, as they increase the ionic strength of the system.[156] Interactions between DES components may also limit the penetration of urea into the protein core, allowing it to interact only with the surface of the protein.[157]

As feathers started to dissolve, all three fractions (regenerated and soluble keratin as well as the unidentified fraction) started to form. At dissolution times greater than 14 h, the amount of regenerated keratin did not increase anymore, while the soluble and unidentified fractions continued to increase, even though the dissolution of the feather was not complete (undissolved feathers were still observed) (Figure 18a). MALDI-TOF MS showed that with a longer dissolution time and at higher temperatures, the keratin molecules started to degrade into smaller-sized fragments (Figure 19a). Most probably, the molecular weight of the smallest keratin molecules was too low for them to aggregate and precipitate when water was added to the system as an anti-solvent to break the interactions between keratin and DES components.

Thus, it appears that NaOAc-urea DES is able to gradually dissolve the feathers and open the structure of keratin as a function of time, but simultaneously keratin is cleaved into smaller fragments (Figure 20).

As the DES dissolution of feather keratin goes on, tight packaging of polypeptides starts to open simultaneously with backbone breakage
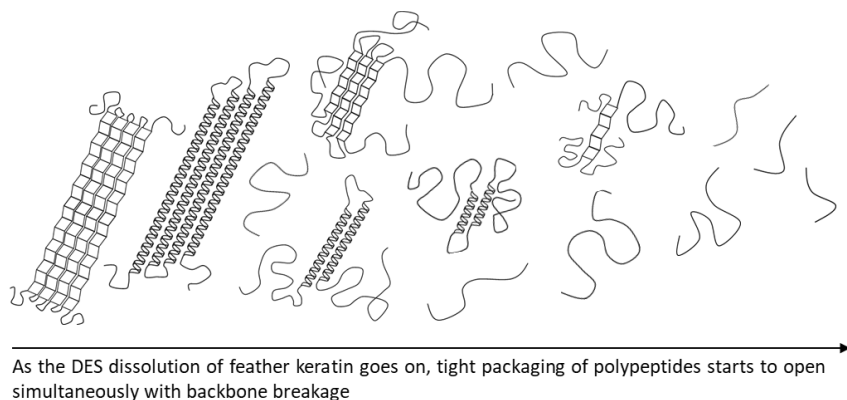
Figure 20. Schematic illustration of a possible scenario for how the native keratin structure of a feather dissolves, its ordered secondary structures open and the polypeptide chain decomposes when dissolved in aqueous DES consisting of NaOAc and urea over time.

4.1.2 Molecular weight of DES-processed molecular keratin

After studying the effect of the dissolution time and temperature of the DES process, it was suggested that the solubility of keratin in water together with the diluted DES components increased as keratin began to lose its molecular weight and ordered conformation. It is well-known that polymer solubility depends on its molecular weight.[158,159] However, the solubility of proteins and peptides is usually a complex process and is affected by many factors. Besides the size[76], the solubility depends on conformation[75], charge[76] and hydrophobicity[76] of the protein.

To ensure enough keratin for further experiments (**publications II & III**), a 15 kg scale DES dissolution (1:3 NaOAc-urea at 95 °C for 7 h) was carried out. Two keratin fractions were obtained: regenerated keratin (high Mw keratin) and soluble keratin (low Mw keratin) (Figure 11). Figure 21 shows the molecular weight distributions of these fractions obtained from MALDI-TOF MS. In regenerated keratin, the high molecular weight peaks at ca. 7000, 8000 and 10,000 m/z were the most intense, while in the soluble fraction, these were present but with substantially lower intensity. In addition to these peaks, several smaller peaks were observed, especially around 4000–6000 m/z. This indicates that the keratin fractions consisted of many different-sized keratin fragments. The spectrum of soluble keratin is wide, with two clearer peaks around 5000 and 5600 m/z. The higher intensities at the smaller mass-to-charge ratios compared to regenerated keratin indicate that the soluble keratin fraction consisted of smaller keratin fragments. Thus, regenerated keratin fraction was called high molecular weight (Mw) keratin, and soluble keratin was called low Mw keratin. A similar division of different fractions has been observed when feathers were dissolved in NMMO and keratin was regenerated with water.[21] In the reported work[21], the fraction that was regenerated after water addition was composed of larger molecules than the fraction that remained soluble. The authors suggested that a part of the keratin may have degraded into individual amino acids.[21] It is obvious that the molecular weight of keratin plays an important role in its fractionation, especially when feathers are processed via chemical routes.
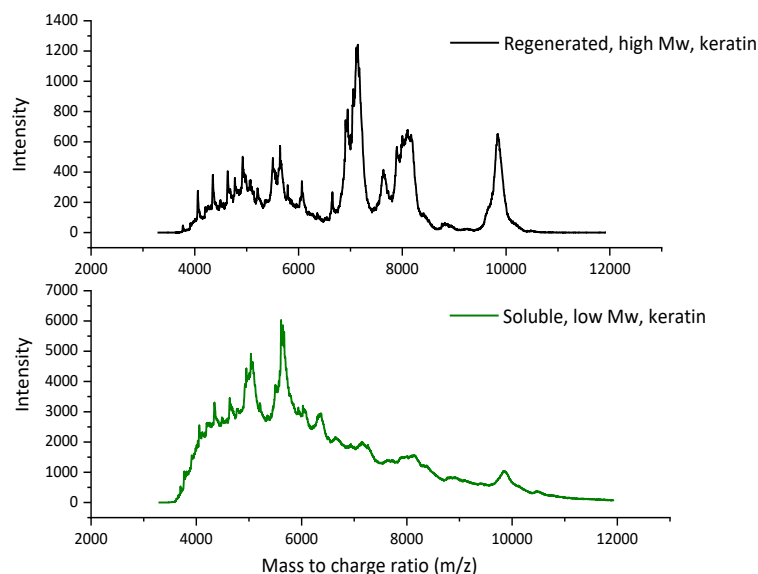
Figure 21. Molecular weight distributions of DES-processed molecular keratin (regenerated and soluble keratin fractions) measured with MALDI-TOF MS (Publication II).

The molecular weight of low Mw keratin was also analysed by SEC (**Publication III**). The weight average molar mass of the low Mw keratin fraction was 4476 ± 71 Da with a polydispersity of 1.7. Although low Mw keratin remained soluble in water together with diluted DES components, after dialysis and freeze-drying, this fraction was not completely soluble in water. This is most likely due to conformational changes that took place during freeze-drying.[160] The weight average molar mass of keratin that was soluble in sodium phosphate buffer (SPB) (pH 7, 150 mM) was only 1192 ± 269 Da with a polydispersity of 1.2, indicating that only the fraction with very low molecular weight was further soluble in SPB. The average molecular weight of an amino acid is 110 Da. Thus, in fact, the keratin fraction soluble in SPB was a peptide rather than a protein because it is about 11 amino acids in length (1192 Da/110 Da = 11). For the low Mw keratin fraction, the results obtained from MALDI-TOF MS and SEC are well in line. The results obtained from SEC analysis complement the suggestion that the fractionation of feather keratin may be strongly dependent on the molecular weight.

4.2 Physical properties of keratin building blocks through film structures

To further understand the difference between the high and low Mw keratin fractions as well as the difference between fibrous and molecular keratin types, self-standing films were prepared and characterized. The effect of plasticizing and cross-linking on film properties is also discussed in this section.

4.2.1 Films prepared from molecular keratin

DES-processed molecular keratin was used to prepare the films (Figure 14, **Publication II**). The films were plasticized with glycerol and cross-linked with glutaraldehyde (GA) and 1.4-butanediol diglycidyl ether (BDE). The mechanical properties and moisture sensitivity were characterized.

4.2.1.1 Comparison of high and low Mw keratin fractions in film structures

To evaluate the potential of high and low Mw keratin fractions in applications, film structures were prepared from both fractions (Figure 14, **Publication II**). The film properties were studied by their morphology, mechanical properties and moisture sensitivity (Table 3), which are all important features for suitability in material applications. The high and low Mw keratin fractions did not differ only in molecular weight but also in conformation. CD spectroscopy revealed that the low Mw keratin fraction had random coil conformation instead of an ordered secondary structure (**Publication III**). The high Mw keratin fraction had a partly ordered secondary structure (**Publication I**).

Plasticizing was needed to ensure sufficient mechanical properties. For low Mw keratin, a concentration of 15 wt% glycerol was not enough to obtain films with sufficient handling properties, while for high Mw keratin, it was enough. Thus, the film comparison between low and high Mw keratin fractions was made with 30 wt% glycerol concentrations. SEM images showed that films made of low Mw keratin had small cracks on the surface (Figure 22a) even after glycerol addition, indicating more fragile films compared to films made of high Mw keratin without cracks on the surface (Figure 22b). Permeable imaging with confocal laser scanning microscopy (CLSM) revealed that films made of low Mw keratin were more homogeneous (Figure 22c) than films made of high Mw keratin that contained particle aggregates (Figure 22d).
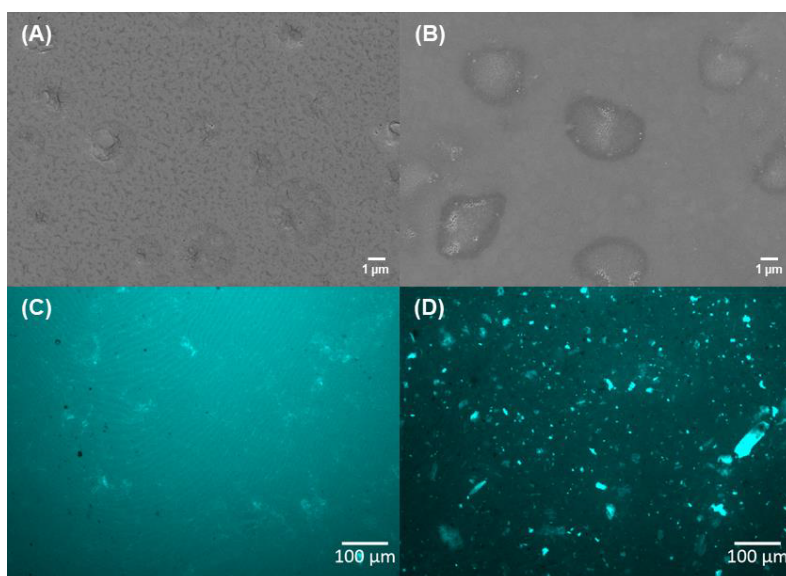
Figure 22. Scanning electron microscopy images of the films made of the (a) low Mw and (b) high Mw keratin fraction with 30 wt% glycerol, and permeable imaging with CLSM of the 30 wt% glycerol plasticized keratin films of the (c) low and (d) high Mw keratin fractions. Adapted from Publication II.

Mechanical testing revealed that the films made of high Mw keratin had better mechanical properties than films made of low Mw keratin (Table 4). The tensile strength, Young's modulus and strain at break values for the films made of the

high Mw keratin fraction were 222%, 158% and 60% higher than the values obtained for the low Mw keratin, respectively. Both the higher molecular weight and the higher degree of ordered secondary structures can explain the better mechanical performance. The mechanical properties of high Mw keratin (2.9 ± 0.2 MPa tensile strength, 48.7 ± 9.0% strain at break, 97.7 ± 24.9 MPa Young's modulus) are comparable to those of glycerol plasticized keratin films and slightly worse than those of glycerol plasticized peanut protein films. In the study of Moore et al.[80], the tensile strength of 2.0 ± 0.2 MPa and the strain at break of 31.9 ± 4.5% with 9% glycerol content have been reported for feather keratin extracted with a reducing agent, while Reddy et al.[160] prepared peanut protein films with 7.5% glycerol content and obtained values of 4.6 ± 0.4 MPa for tensile strength and 66 ± 16% for strain at break and 102 ± 18 MPa for modulus.

The moisture sensitivity of both films was determined by measuring their WVP (Table 4). The films made of low Mw keratin showed 98% lower WVP values compared to high Mw keratin. Most probably, a low Mw keratin fraction allowed tighter packaging of keratin molecules in the film network, thus allowing the lower permeability since a denser molecule matrix decreases permeability.[161] Keratin has a hydrophilic nature, and the addition of small hydrophilic glycerol molecules in the film structure not only makes the film even more hydrophilic but also increases the mobility and the free volume between the keratin chains, making the films even more prone to water adsorption.[108] However, the WVP values obtained for the films made of DES fractionated keratin are lower ($0.005 \pm 0.0003 \cdot 10^{-10}$ g m m^{-2} s^{-1} Pa^{-1}) than previously reported glycerol plasticized feather keratin films ($35.5 \cdot 10^{-10}$ g m m^{-2} s^{-1} Pa^{-1} [102] and $3.5 \cdot 10^{-10}$ g m m^{-2} s^{-1} Pa^{-1} [162]).

It is concluded that the high Mw keratin fraction gave better mechanical properties due to the higher molecular weight and ordered secondary structures compared to low Mw keratin. However, due to the absence of ordered structures and lower molecular weight, low Mw keratin was able to form a more homogenous and denser film network, leading to better WVP values compared to those of high Mw keratin.

Table 4. The measured mechanical properties, WVP, solubility, swelling and contact angle for molecular keratin films plasticized with glycerol and cross-linked with BDE.

	Tensile Strength (MPa)	Young's Modulus (MPa)	Strain at Break (%)	WVP ($\times 10^{-10}$ g m m^{-2} s^{-1} Pa^{-1})	Solubility (%)	Swelling (%)		Contact angle (°)
						75% RH	90% RH	
Low Mw keratin with 30 wt% glycerol	0.9 ± 0.1	38.4 ± 5.5	30.4 ± 5.8	0.005 ± 0.0003	-	-	-	-
Low Mw keratin cross-linked with BDE	1.5 ± 0.1	16.0 ± 4.0	51.0 ± 6.0	0.04 ± 0.03	-	-	-	-
High Mw keratin with 15 wt% glycerol	8.4 ± 0.9	649.1 ± 28.8	1.7 ± 0.2	0.04 ± 0.01	-	19.7 ± 10.0	23.0 ± 0.7	45.8 ± 4.6
High Mw keratin with 30 wt% glycerol	2.9 ± 0.2	97.7 ± 24.9	48.7 ± 9.0	0.2 ± 0.02	-	5.9 ± 5.6	32.7 ± 0.9	61.0 ± 0.3
High Mw keratin cross-linked with BDE	4.7 ± 0.3	53.0 ± 11.0	65.0 ± 4.0	0.2 ± 0.09	42.3 ± 6.3	8.8 ± 0.5	21.4 ± 0.4	91.0 ± 0.3

4.2.1.2 The effect of plasticizing and cross-linking

The need for plasticizers in keratin films is well-known.[23,80,91,106–109] Glycerol was used to plasticize high and low Mw keratin films (Figure 14, **Publication II**). When the concentration of glycerol in high Mw keratin films increased from 15 to 30% by weight, the tensile strength and Young's modulus of the films decreased by 65% and 85%, the strain at break increased by 2765% and they became more sensitive to moisture as WVP values and swelling increased by 400% and 50%, respectively. The effect of the plasticizing was expected from the literature since when introducing small hydrophilic glycerol molecules inside the film network, protein-protein interactions are disturbed and the free volume increases.[163]

Films were also cross-linked with glutaraldehyde (GA) and 1.4-butanediol diglycidyl ether BDE (Figure 14). Although both cross-linkers showed some effect on the film properties, GA did not show a clear cross-linking effect unlike BDE, which was able to form new interactions within the film network. While the reaction including BDE takes place between the epoxy and the amino groups and involves the ring-opening of the epoxy[164,165], GA reacts with the amino groups of lysine[110,166]. However, the lysine content in feather keratin is low[21], which could explain the low degree of cross-linking. Figure 23 shows the suggested cross-linking reaction with BDE.
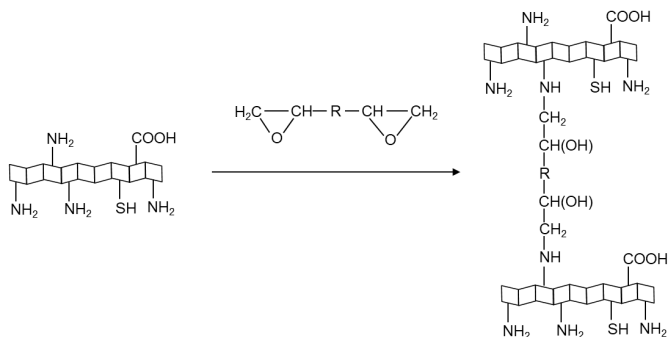
Figure 23. Suggested reaction when keratin is cross-linked with BDE.

NMR and ATR-FTIR both showed indications of successful cross-linking with BDE (**Publication II**). In ^{1}H-NMR spectra of BDE cross-linked low Mw keratin films, the intensity of the peaks assigned to the amide protons of the glycine, asparagine and glutamine residues[167] decreased, indicating the possible reaction of amides with BDE. In ATR-FTIR spectra of BDE cross-linked keratin films, the relative intensity ratio between the amide II band at $1480–1570$ cm^{-1} (NH bending and CH stretching vibrations) and the amide I band at $1600–1700$ cm^{-1} (C=O stretching) increased compared to samples without cross-linking, which may be due to changes in amine vibration after cross-linking. Besides these effects, no major changes in the keratin chemical structure took place during the cross-linking according to the NMR and ATR-FTIR spectra.

SEM imaging revealed that the surface morphology of the films became rougher and more heterogeneous after the BDE cross-linking, indicating some rearrangements of the keratin molecules (**Publication II**). Table 4 shows the

changes in the mechanical properties after the cross-linking. After the BDE addition, the tensile strength of the films made of the high Mw keratin fraction increased by 62% and the strain at break by 33%, while Young's modulus decreased by 46%. In the films made of the low Mw keratin fraction, the tensile strength increased by 67%, the strain at break by 68% and Young's modulus decreased by 58%. Although improvements in strength properties could be explained by the new cross-links within the network, the increase in the strain at break is related more to the plasticizing effect. It has been suggested that BDE can have a plasticizing effect due to hydroxyl groups and hydroxyl-terminated pendant groups from the hydrolyzed un-reacted epoxides.[164]

For high Mw keratin, WVP values did not show a significant difference before and after cross-linking with BDE, while for low Mw keratin, a slight increase was detected (Table 4). Although it is assumed that cross-linking can make the film network denser and thus improve its permeability properties[161,164], it was noticed that BDE had also a plasticizing effect, which, in turn, might repeal this effect. Moreover, it is also suggested that accumulated water molecules in the protein network can act as a plasticizer.[168] The WVP value of the BDE cross-linked gelatin film ($0.197 \cdot 10^{-10}$ g m -2 s^{-1} Pa^{-1}) has been reported to be in a similar range.[164]

When immersed in water, films without cross-linking disintegrated. Only the cross-linked films made of the high Mw keratin fraction remained intact. But also in these cases, approximately 40% of the film weight disintegrated in water (Table 4). Cross-linking has been reported to decrease the solubility of feather keratin[162] and other protein films[161,168] in water, and it has been suggested that in the cross-linked network, proteins interact less with water molecules[162]. The films in this study contained 30 wt% glycerol as a plasticizer, which means that not only the small glycerol molecules exudated out of the films. From MALDI-TOF MS data, it was seen that the DES-fractionated keratin consisted of many different sizes of keratin fragments (Figure 21). Thus, it is likely that besides glycerol, the keratin fragments with the lower molecular weight disintegrated from the film structure. The low molecular weight of low Mw keratin could also explain why the films made of the low Mw keratin did not remain intact even after cross-linking.

Water acts as a strong plasticizer in hydrophilic films by accumulating in the structure.[162] The swelling of the films was followed by the increase in relative humidity (RH), first from 50% to 75% and then to 90%. The films made of the low Mw keratin became too gel-like to remain intact during the measurement. Thus, the swelling could be measured only for the films made of the high Mw keratin with and without the cross-linking (Table 4). Except for the BDE cross-linked films, a significant dispersion in the results indicates that the films without the cross-linker were not uniform. The BDE cross-linked films showed a smaller scatter between parallel samples, which could indicate that BDE was able to form a more uniform cross-linked keratin network in comparison to the films without the cross-linker. At 90% relative humidity, the BDE cross-linked film swelled only 21.42 ± 0.47%, while the films without the cross-linking swelled 32.73 ± 0.86%. Also, in the study by Martucci *et al.*[164], the swelling of

the gelatin films decreased from 18% to 11% when the gelatin was cross-linked with BDE. It is speculated that cross-linking forms a network in which the hydrophilic groups in the protein are not available for water sorption, thus decreasing the moisture content in the films. However, at the same time, BDE contains hydroxyl groups that can bind to water.[162]

In WCA measurements, the films cross-linked with BDE showed hydrophobicity with low scattering (90.95 ± 0.32, Table 4), again indicating that the addition of BDE formed a more uniform surface in which hydrophilic groups were not exposed. All the samples, except the films cross-linked with BDE, had a WCA value below 90 °, indicating that the surfaces of the films were wetted (Table 4).

It can be concluded that a dense and uniform keratin network together with high molecular weight is recommended to ensure good film properties (mechanical properties and properties related to interactions with water and moisture). However, these properties can also be controlled by plasticizing and cross-linking. Protein films of this type can be used for food packaging or medical applications such as wound care.

4.2.2 Comparison of molecular and fibrous keratin films

While the DES process was used to generate molecular keratin, alkaline pretreated and milled feathers (Figure 12, **Publication IV**) were considered as fibrous keratin. Both molecular and fibrous keratin were used to prepare films to allow comparison (Figure 14, Figure 15, **publications II and IV**). The films were compared by their uniformity and mechanical properties and how well these properties could be modified with additives (Table 3).

Both films were prepared by the solvent-casting method from keratin suspensions. While molecular keratin formed a fine dispersion with small particles (Figure 24a), fibrous keratin included stiff and sharp fibres together with round-shaped fines (Figure 24b). While films prepared from fibrous keratin were opaque due to light scattering in a porous film structure (Figure 24d), films made of molecular keratin were transparent (Figure 24c). SEM images revealed that films made of fibrous keratin had a structure consisting of randomly oriented, relatively stiff, flat fibers together with more round-shaped fines (Figure 24f), while molecular keratin allowed rather smooth film formation (Figure 24e).

Like films made of molecular keratin, films made of fibrous keratin were also fragile without any additives. A variety of different additives were tested (**Publication IV**). The strongest films were obtained with maleic acid, sorbitol and ethanolamine as single additives, while sodium alginate as a secondary additive with ethanolamine had a positive impact on tensile strength with and without cationic metal ions used to crosslink sodium alginate. The films were also plasticized with 20% glycerol, and the values obtained from the mechanical testing were in a similar range together with the films made of molecular keratin which were plasticized with 15% glycerol.

Although the addition of additives was essential to improve the film formation of fibrous keratin, the impact of additives was rather modest in the mechanical properties. It seems that the porous film structure had a dominating role and

the stiff fibers had limited reactivity toward additives. Compared to fibrous keratin, molecular keratin showed better reactivity, and the effect of plasticizers and cross-linker had a clear effect on the properties.

Alkaline pre-treatment, together with milling, was used to process feathers as a simpler and less expensive alternative for the DES process. Although molecular keratin is more suitable in most applications, it is suggested that fibrous keratin could be used in applications in which a more native feather structure is preferred and transparency, good barrier properties or reactivity are not essential in biocomposites, non-wovens, and fibre boards.[43,44,169,170]
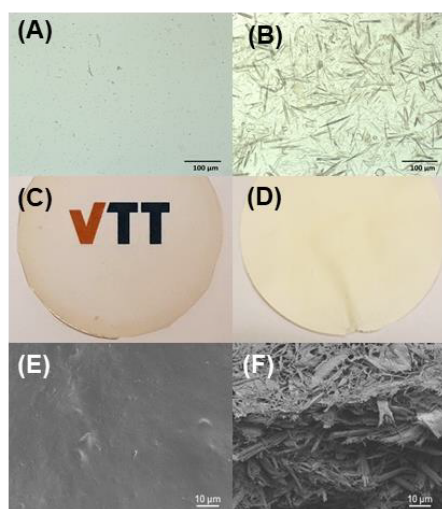

Figure 24. Images of (a,c,e) molecular and (b,d,f) fibrous keratin when used in film structures. Light microscopy images of (a,b) aqueous suspensions, images of (c,d) films prepared for those suspensions and SEM images of (e,f) their macroscale structures. Adapted from publications II and IV.

4.3   Interactions of keratin peptides with lignocellulosic materials

Keratin could bring additional properties to lignocellulosic materials, making them more suitable for the medical, cosmetic, electronics, agriculture, textile and composite industries.[5] To obtain a fundamental understanding of this kind of combination, keratin adsorption on thin films made of cellulose and lignin was studied using the QCM-D technique (**Publication III**). The results are summarized and discussed in this section. The keratin used in these adsorption studies was obtained from the DES process (Figure 11), and the fraction that was further soluble in buffers was used. After characterization with SEC, CD and zeta sizer (Table 3), it was found that this buffer-soluble keratin fraction was a peptide (Mw about 1000 Da) with a random coil conformation and an isoelectric point (IEP) at pH 3. A random coil conformation makes this keratin fraction labile, and it is able to unfold upon adsorption to adopt a conformation that is favourable for adsorption.[141]

4.3.1 Interactions between keratin and lignocellulosic materials

The frequency changes (Δf_3 values) upon keratin adsorption on thin films made of cellulose, lignin or colloidal lignin particles (CLPs) revealed that the lignin and CLP substrates exhibited high keratin adsorption, while on a cellulose substrate, keratin had low adsorption (Figure 25). Changes in dissipation (ΔD_3 values) after keratin adsorption onto lignin and cellulose indicated that small keratin peptides were rigidly adsorbed on surfaces, and dense films formed. On the other hand, the ΔD_3 value for the CLP substrate was negative, indicating that the film on the sensor became denser, although the mass on the CLP substrate increased after the keratin adsorption. The decrease in dissipation is related to the release of bound water from CLPs upon the adsorption of keratin.[135,147,171]

Peptide adsorption on a solid substrate is affected by the properties of the peptide, substrate and surrounding medium. Protein adsorption is often explained by attraction between opposite charges or increased entropy due to either released solvent molecules from the surfaces or changes in the conformation of the protein upon adsorption.[141,143] At pH 7, keratin peptide (IEP at pH 3) as well as cellulose[172] and lignin surfaces[173] had a negative net surface charge, which could suggest that the long-range electrostatic attraction between the oppositely charged molecules did not dominate the adsorption. However, it must be noted that at pH 7, some amino acids, such as glutamine, lysine and arginine, also carry a positive charge which could allow attractive long-range electrostatic interactions with negatively charged groups. However, the adsorption on cellulose was low despite this possibility. One explanation for this could be the lower negative charge of cellulose[172] compared to lignin[173].

It has been reported that the water contact angle (WCA) of regenerated cellulose is 31° ± 3°.[172] This indicates a hydrophilic surface, which could explain the absence of strong hydrophobic interactions and entropy gain and the poor adsorption of keratin on cellulose. Furthermore, it is reported that the WCA of lignin thin film made of dissolved lignin is 63° ± 2°[129], which could explain the hydrophobic interactions and entropy gain due to release of ordered water molecules at the surfaces. However, the contact angle of the CLP surface has been reported to be only 17° ± 1°[129], and the keratin adsorption on the CLP surface was higher than on lignin and much higher than on cellulose, suggesting that hydrophobic interactions did not alone drive keratin adsorption.

It is suggested that the keratin peptides contained amino acids that are able to interact with lignin, while the random coil conformation of keratin peptides enabled these residues to be appropriately arranged in relation to the binding site in lignin. Peptides that contain histidine, phenylalanine, proline, and serine residues have been reported to have a high affinity for lignin surfaces.[146] More detailed, protein adsorption on lignin has been suggested to take place via short-range interactions between the aromatic moieties of lignin and proline.[138] Soluble feather keratin is relatively rich in proline and serine.[21] The higher adsorption onto a CLP thin film compared to dissolved lignin could be explained by the higher available surface with CLPs[129] and the higher degree of dehydration (as seen from ΔD_3 values in Figure 25), which increase the entropy of the system. Moreover, CLPs have more accessible carboxyl and hydroxyl groups on their

surface, which could allow more favourable interactions with keratin. However, it is also suggested that cellulose thin films are in an amorphous state, which means that the hydroxyl groups of cellulose are available.[123,125] As the adsorption on cellulose was low, it seems that the hydroxyl groups were not driving the adsorption, but the interactions between the carboxyl groups of CLPs and keratin cannot be excluded. The adsorption of proteins onto cellulose surfaces usually takes place via specific cellulose-binding domains (CBDs)[174] that seem to be absent in the DES-processed keratin peptides.
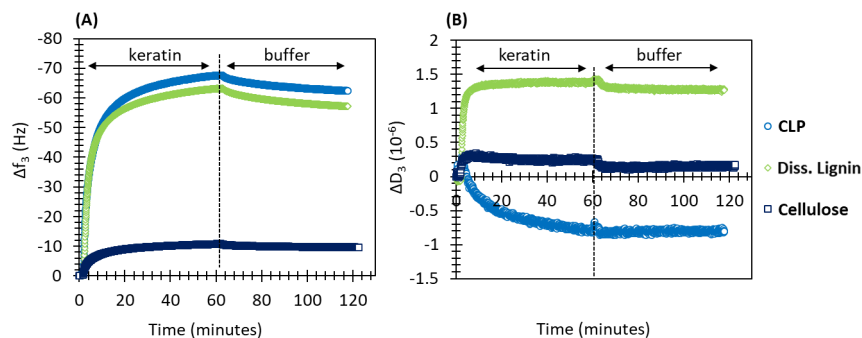

Figure 25. QCM-D detection of the adsorption of keratin onto CLP, dissolved (diss.) lignin and cellulose model films: (A) frequency and (B) dissipation changes vs. time at the third overtone. Adapted from Publication III.

4.3.2 The effect of pH and ionic strength on keratin adsorption

The conditions in the surrounding medium were altered in a controlled manner to further understand the adsorption behaviour. On lignin substrates, keratin had high adsorption, and the adsorption behaviour could be modified by altering the pH and ionic strength of the aqueous media, while adsorption on cellulose was not affected by these changes. Figure 26 shows the sensed mass calculated from the Sauerbrey equation as a function of the ionic strength and pH. Quite surprisingly, the adsorbed mass was lowest when the electrostatic interactions were screened (high ionic strength or pH 3 when the net surface charge of keratin was zero) and highest when both keratin and lignin had a negative net surface charge. Moreover, at the lowest ionic strength of 50 mM, the dissipation changes were the largest, indicating that the adsorbed films on both lignin (ΔD = 4.0 · 10^{-6}) and CLP films (ΔD = 2.3 · 10^{-6}) were the most hydrated and swollen (**Publication III**).

It was expected that at pH 3 or high ionic strengths, the adsorption of keratin would have been higher than at higher pHs or low ionic strengths because long-range electrostatic interactions were screened, allowing a larger amount of protein to accommodate at the surface.[143] Despite the negative net charge, some amino acids in keratin can have a positive charge even at pH 7, which could allow for specific attractive electrostatic interactions with carboxyl groups in lignin. As the pH increases from 3 to 7, lignin gets even more groups negatively charged, which could interact with the amino acids carrying a positive charge. However, the electrostatic double layer force is still repulsive since the counterion distribution will be defined by the net charge. Moreover, the solubility of

keratin depends on its molecular weight, and the solubility varied a lot depending on the pH and salt concentration of the buffer solution. At low ionic strengths and high pHs, keratin fragments with a higher molecular weight were dissolved. It has been suggested that polymer adsorption increases and becomes more favourable when the molecular weight of the polymer increases.[144] This is explained by a decreased loss of entropy on polymer adsorption when the molecular weight increases. Simpler systems like peptides have been found to follow this prediction, while in more complex systems such as polyelectrolytes and proteins, other factors dominate over molecular weight in adsorption.[144] It is also speculated that molecules with higher molecular weight or extended conformation may have higher adsorption onto surfaces due to the higher number of available sites[175], which also includes hydrophobic and positively charged amino acids. Thus, it can be speculated that the increased adsorbed keratin mass at higher pHs and lower ionic strengths could be explained by the structural properties of keratin, but also the electrostatic interactions are suggested to have a role.
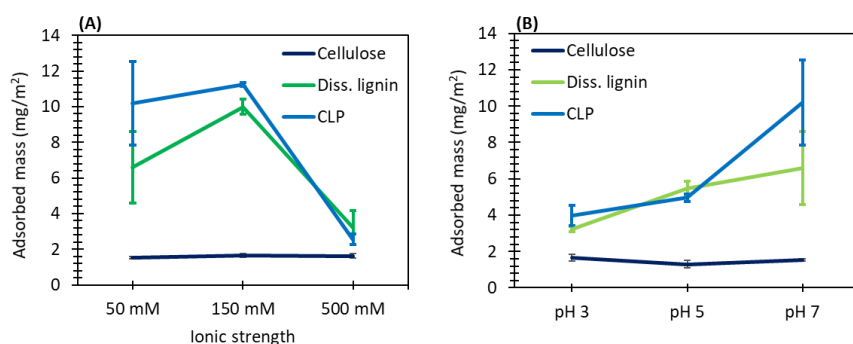
Figure 26. Adsorption of keratin calculated from the Sauerbrey equation on CLPs, lignin and cellulose model films at different (A) ionic strengths and (B) pHs. Adapted from Publication III.

It was observed that the adsorption of keratin on lignin is a complex process. But it is anticipated that the structure, especially the conformation, amino acid content and molecular weight of keratin played an important role. Figure 27 summarizes the interpretations made of the DES-treated feather keratin on lignin surfaces based on the QCM-D studies. When the long-range electrostatic interactions were not present (screened by high ionic strength or at pH close to the IEP of keratin), adsorption of keratin was minor, and adsorbed layers were not very hydrated. However, when the long-range electrostatic interactions were present (both keratin and lignin had a negative net charge, but keratin had also positively charged groups), more and larger keratin molecules were adsorbed, and the adsorbed layer was more hydrated and extended.
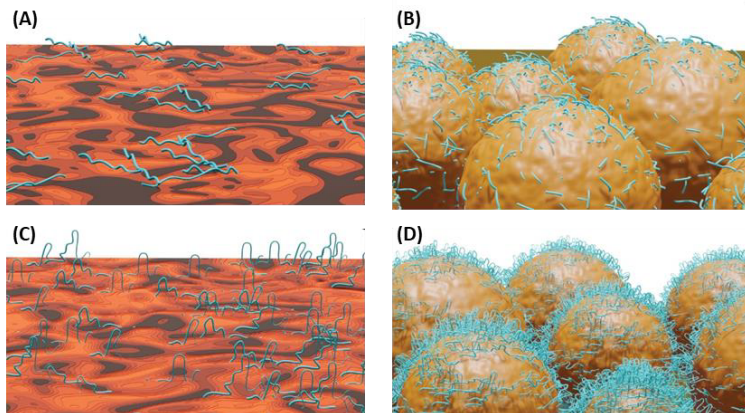
Figure 27. Illustrative schematics summarizing the main observations regarding the adsorption of keratin peptides on (A) surfaces made of dissolved lignin when the long-range electrostatic repulsion is screened or keratin is non-charged, (B) CLP surfaces when the electrostatic interactions are screened or keratin is non-charged, (C) surfaces made of dissolved lignin when both keratin and lignin have a negative net charge and (D) CLP surfaces when both keratin and lignin have a negative net charge. Adapted from Publication III.

5. Concluding remarks

Considering the replacement of fossil-based materials, and the aspects of resource sufficiency and the circular economy, valourization of feather keratin should not be ignored.

This thesis demonstrated how feathers can be converted into utilizable keratin fractions, and it evaluated their potential as building blocks for macro- and nanoscale material applications. Overall, the thesis showed the importance of choosing the processing method and how the structural and physical properties of the feather keratin as well as its interactions with lignocellulosics can be affected when keratin is produced for material applications.

For most applications, feathers require processing, and the choice of the method to process feathers greatly depends on the intended application. The morphology, as well as the molecular weight of keratin, play a critical role when the applicability of keratin is considered. Molecular keratin can be produced via chemical routes, and the powdered and soluble forms of the molecular keratin allow their utilization in a variety of applications, including biomedical, packaging, cosmetic, textile and electronic applications. While molecular keratin with low molecular weight is suitable in applications in which solubility and a random coil conformation are preferred, some polymeric structures like films and filaments would require keratin with higher molecular weight and ordered secondary structures. Although molecular keratin is more suitable for applications in which transparency, good barrier properties or reactivity are essential, fibrous keratin prepared via simpler mechanical routes could be used in applications in which more native feather structure is beneficial, for example in biocomposites, non-wovens and fibre boards.

Although keratin could be suitable as a main component in material applications, combining keratin with other materials, especially cellulose and lignin, is an attractive approach to achieve materials with sufficient properties to compete with the fossil-based alternatives. Interactions between lignin and keratin are good, while the interactions between cellulose and keratin should be improved, for example, by covalently cross-linking them together or using cellulosic materials where lignin is not removed. Keratin combined with colloidal lignin nanoparticles appears as an especially interesting approach because the spherical morphology of the nanoparticles is beneficial in many practical applications such as hydrogels and coatings.

The potential of side-stream feather keratin should be recognized more widely since its utilization in material applications would offer new essential and significant improvements to the growing range of bio-based materials. The commercialization of feather keratin in material applications still requires consistent research work that would include the identification of the aimed application and optimizing the process to produce the keratin. Also, life cycle, life cycle cost and social life cycle assessments as well as market analysis for intended applications would be required.

6. References

1. Statista. Annual production of plastics worldwide from 1950 to 2020. https://www.statista.com/statistics/282732/global-production-of-plastics-since-1950/. (Accessed 5.3.2022)

2. Statista. Global chemical fiber production from 2000 to 2020, by fiber type. https://www.statista.com/statistics/271651/global-production-of-the-chemical-fiber-industry/. (Accessed 5.3.2022)

3. Eurostat. Agricultural production - livestock and meat. https://ec.europa.eu/eurostat/statistics-explained/index.php?title=Agricultural_production_-_livestock_and_meat&oldid=549389#Poultrymeat. (Accessed 5.3.2022)

4. Williams, C. M. Poultry Development Review. 60, *Food and Agriculture Organization of the United Nations* (2013). ISBN 978-92-5-108067-2

5. Reddy, N. Non-food industrial applications of poultry feathers. *Waste Manag.* **45**, 91–107 (2015).

6. Barone, J. R., Schmidt, W. F. & Gregoire, N. T. Extrusion of feather keratin. *J. Appl. Polym. Sci.* **100**, 1432–1442 (2006).

7. Cepi. *KEYSTATISTICS 2020 European pulp & paper industry*. https://library.cepi.org. (Accessed 5.3.2022)

8. Shavandi, A., Silva, T. H., Bekhit, A. A. & Bekhit, A. E. D. A. Keratin: Dissolution, extraction and biomedical application. *Biomater. Sci.* **5**, 1699–1735 (2017).

9. Prum, R. O. Development and evolutionary origin of feathers. *J. Exp. Zool.* **285**, 291–306 (1999).

10. McKittrick, J. *et al.* The structure, functions, and mechanical properties of keratin. *JOM.* **64**, 449–468 (2012).

11. Reddy, N. & Yang, Y. Structure and properties of chicken feather barbs as natural protein fibers. *J. Polym. Environ.* **15**, 81–87 (2007).

12. Tesfaye, T., Sithole, B., Ramjugernath, D. & Chunilall, V. Valorisation of chicken feathers: Characterisation of chemical properties. *Waste Manag.* **68**, 626–635 (2017).

13. Lingham-Soliar, T., Bonser, R. H. C. & Wesley-Smith, J. Selective biodegradation of keratin matrix in feather rachis reveals classic bioengineering. *Proc. R. Soc. B Biol. Sci.* **277**, 1161–1168 (2010).

14. Fraser, R. D. B. & Parry, D. A. D. The structural basis of the filament-matrix texture in the avian/reptilian group of hard β-keratins. *J. Struct. Biol.* **173**, 391–405 (2011).

15. Feughelman, M. Natural protein fibers. *J. Appl. Polym. Sci.* **83**, 489–507 (2001).

16. Schmidt, W. F. & Jayasundera, S. (Edited by Wallenberger, F.T. and Weston, N.) Natural Fibers, Plastics and Composites. 370, *Kluwer Academic Publishers* (2004). ISBN 1-4020-7643-6

17. Chou, P. Y. & Pasman, G. D. Conformational Parameters for Amino Acids in Helical, β-Sheet, and Random Coil Regions Calculated from Proteins. *Biochemistry* **13**, 211–222 (1974).

18. Arai, K. M., Takahashi, R., Yokote, Y. & Akahane, K. Amino-Acid Sequence of Feather Keratin from Fowl. *Eur. J. Biochem.* **132**, 501–507 (1983).

19. Filshie, B. K. & Rogers, G. E. An electron microscope study of the fine structure of feather keratin. *J. Cell Biol.* **13**, 1–12 (1962).

20. Numata, K. How to define and study structural proteins as biopolymer materials. *Polym. J.* **52**, 1043–1056 (2020).

21. Ma, B., Sun, Q., Yang, J., Wizi, J., Hou, X. & Yang, Y. Degradation and regeneration of feather keratin in NMMO solution. *Environ. Sci. Pollut. Res.* **24**, 17711–17718 (2017).

22. Yin, J., Rastogi, S., Terry, A. E. & Popescu, C. Self-organization of oligopeptides obtained on dissolution of feather keratins in superheated water. *Biomacromolecules* **8**, 800–806 (2007).

23. Yin, X. C., Li, F. Y., He, Y. F., Wang, Y. & Wang, R. M. Study on effective extraction of chicken feather keratins and their films for controlling drug release. *Biomater. Sci.* **1**, 528–536 (2013).

24. Fraser, R. D. B. & Parry, D. A. D. Molecular packing in the feather keratin filament. *J. Struct. Biol.* **162**, 1–13 (2008).

25. Zhao, W., Yang, R., Zhang, Y. & Wu, L. Sustainable and practical utilization of feather keratin by an innovative physicochemical pretreatment: High density steam flash-explosion. *Green Chem.* **14**, 3352–3360 (2012).

26. Wang, J., Hao, S., Luo, T., Yang, Q. & Wang, B. Development of feather keratin nanoparticles and investigation of their hemostatic efficacy. *Mater. Sci. Eng. C* **68**, 768–773 (2016).

27. Chaitanya, C., Ahamad, I., Gupta, A. & Bhuyar, P. Valorization of keratin waste biomass and its potential applications. *J. Water Process Eng.* **40**, 101707 (2021).

28. Wang, J., Hao, S., Luo, T., Cheng, Z., Li, W., Gao, F., Guo, T., Gong, Y. & Wang, B. Colloids and Surfaces B : Biointerfaces Feather keratin hydrogel for wound repair : Preparation , healing effect and biocompatibility evaluation. *Colloids Surfaces B Biointerfaces* **149**, 341–350 (2017).

29. Xu, H., Cai, S., Xu, L. & Yang, Y. Water-Stable Three-Dimensional Ultrafine Fibrous Scaffolds from Keratin for Cartilage Tissue Engineering. *Langmuir* **30**, 8461-8470 (2014).

30. Wang, X., Lu, C. & Chen, C. Effect of Chicken-Feather Protein-Based Flame Retardant on Flame Retarding Performance of Cotton Fabric. *J. Appl. Polym. Sci.* **2014**, 1–8 (2014).

31. Hu, P. Zheng, X., Zhu, J. & Wu, B. Effects of chicken feather keratin on smoke suppression characteristics and flame retardancy of epoxy resin. *Polym. Adv. Technol.* **31**, 2480–2491 (2020).

32. Barba, C., Méndez, S., Roddick-Lanzilotta, A., Kelly, R., Parra, J. & Coderch, L. Cosmetic effectiveness of topically applied hydrolysed keratin peptides and lipids derived from wool. *Ski. Res. Technol.* **14**, 243–248 (2008).

33. Cataldi, P., Condurache, O., Spirito, D., Krahne, R., Bayer, I., Athanassiou, A. & Pertto, G. Keratin-Graphene Nanocomposite: Transformation of Waste Wool in Electronic Devices. *ACS Sustainable Chem. Eng.* **7**, 12544-12551 (2019).

34. Song, K., Xu, H., Xu, L., Xie, K. & Yang, Y. Bioresource Technology Cellulose nanocrystal-reinforced keratin bioadsorbent for effective removal of dyes from aqueous solution. *Bioresour. Technol.* **232**, 254–262 (2017).

35. Aluigi, A., Corbellini, A., Rombaldoni, F. & Mazzuchetti, G. Wool-derived keratin nanofiber membranes for dynamic adsorption of heavy-metal ions from aqueous solutions. *Textile Research Journal* **83**, 1574-1586 (2013).

36. Zhou, L. & Guang, Y. Preparation of regenerated keratin sponge from waste feathers by a simple method and its potential use for oil adsorption. *Environ. Sci. Pollut. Res.* 21, 5730–5736 (2014).

37. Idris, A., Vijayaraghavan, R., Rana, U., Fredericks, D., Patti, A. & MacFarlane, D. Dissolution of feather keratin in ionic liquids. *Green Chem.* **15**, 525–534 (2013).

38. Verbeek, C. J. R. & Berg, L. E. van den. Recent Developments in Thermo-Mechanical Processing of Proteinous Bioplastics. *Recent Patents Mater. Sci.* **2**, 171–189 (2010).

39. Barakat, A., Vries, H. De & Rouau, X. Dry fractionation process as an important step in current and future lignocellulose biorefineries : A review. *Bioresour.*

Technol. **134**, 362–373 (2013).

40. Barakat, A., Mayer-Laigle, C., Solhy, A., Arancon, R., Vries, H. & Luque, R. Mechanical pretreatments of lignocellulosic biomass: Towards facile and environmentally sound technologies for biofuels production. *RSC Adv.* **4**, 48109–48127 (2014).

41. Huda, S. & Yang, Y. Composites from ground chicken quill and polypropylene. *Compos. Sci. Technol.* **68**, 790–798 (2008).

42. Pourjavaheri, F., Jones, O., Mohaddes, F., Sherkat, F., Gupta, A. & Shanks, R. Green plastics: Utilizing chicken feather keratin in thermoplastic polyurethane composites to enhance thermo-mechanical properties. *Annu. Tech. Conf. - ANTEC, Conf. Proc.* 398–405 (2016).

43. Aranberri, I., Montes, S., Azcune, I., Rekondo, A. & Grande, H. J. Fully biodegradable biocomposites with high chicken feather content. *Polymers* **9**, 593-602 (2017).

44. Aranberri, I., Montes, S., Azcune, I., Rekondo, A. & Grande, H. J. Flexible biocomposites with enhanced interfacial compatibility based on keratin fibers and sulfur-containing poly(urea-urethane)s. *Polymers* **10**, 1–14 (2018).

45. Barone, J. R., Schmidt, W. F. & Liebner, C. F. E. Thermally processed keratin films. *J. Appl. Polym. Sci.* **97**, 1644–1651 (2005).

46. Pedram Rad, Z., Tavanai, H. & Moradi, A. R. Production of feather keratin nanopowder through electrospraying. *J. Aerosol Sci.* **51**, 49–56 (2012).

47. Zhang, Y., Zhao, W. & Yang, R. Steam Flash Explosion Assisted Dissolution of Keratin from Feathers. *ACS Sustain. Chem. Eng.* **3**, 2036–2042 (2015).

48. Zhang, Y., Yang, R. & Zhao, W. Improving digestibility of feather meal by steam flash explosion. *J. Agric. Food Chem.* **62**, 2745–2751 (2014).

49. Senoz, E., Stanzione, J. F., Reno, K. H., Wool, R. P. & Miller, M. E. N. Pyrolyzed chicken feather fibers for biobased composite reinforcement. *J. Appl. Polym. Sci.* **128**, 983–989 (2013).

50. Belarmino, D., Ladchumananandasivam, R., Belarmino, L., Pimental, J., Rocha, B., Galvão, A. & Andrade, S. Physical and Morphological Structure of Chicken Feathers (Keratin Biofiber) in Natural, Chemically and Thermally Modified Forms. *Mater. Sci. Appl.* **3**, 887–893 (2012).

51. Schrooyen, P. M. M., Dijkstra, P. J., Oberthü, R. G., Bantjes, A. & Feijen, J. Partially carboxymethylated feather keratins. 1. Properties in aqueous systems. *J. Agric. Food Chem.* **48**, 4326–4334 (2000).

52. Sayyed, A. J., Deshmukh, N. A. & Pinjari, D. V. A critical review of manufacturing processes used in regenerated cellulosic fibres: viscose, cellulose acetate, cuprammonium, LiCl/DMAc, ionic liquids, and NMMO based lyocell. *Cellulose* **26**, 2913–2940 (2019).

53. Rosenau, T., Potthast, A., Sixta, H. & Kosma, P. The chemistry of side reactions and byproduct formation in the system NMMO/cellulose (Lyocell process). *Prog. Polym. Sci.* **26**, 1763–1837 (2001).

54. Brandt, A., Gräsvik, J., Hallett, J. P. & Welton, T. Deconstruction of lignocellulosic biomass with ionic liquids. *Green Chem.* **15**, 550–583 (2013).

55. Sixta, H., Michud, A., Hauru, L., Asaadi, S., Ma, Y., King, A., Kilpeläinen, I. & Hummerl, M. Ioncell-F: A high-strength regenerated cellulose fibre. *Nord. Pulp Pap. Res. J.* **30**, 43–57 (2015).

56. Zhu, S., Wu, Y., Chen, Q., Yu, Z., Wang, C., Jin, S., Ding, Y. & Wu, G. Dissolution of cellulose with ionic liquids and its application: A mini-review. *Green Chem.* **8**, 325–327 (2006).

57. Sun, P., Liu, Z. T. & Liu, Z. W. Particles from bird feather: A novel application of an ionic liquid and waste resource. *J. Hazard. Mater.* **170**, 786–790 (2009).

58. Wang, Y. X. & Cao, X. J. Extracting keratin from chicken feathers by using a hydrophobic ionic liquid. *Process Biochem.* **47**, 896–899 (2012).

59. Idris, A., Vijayaraghavan, R., Patti, A. F. & Macfarlane, D. R. Distillable protic ionic liquids for keratin dissolution and recovery. *ACS Sustain. Chem. Eng.* **2**, 1888–1894 (2014).

60. Kammiovirta, K., Jääskeläinen, A., Kuutti, L., Holopainen-Mannila, U., Paananen, A., Suurnäkki, A. & Orelma, H. Keratin-reinforced cellulose filaments from ionic liquid solutions. *RSC Adv.* **6**, 88797–88806 (2016).

61. De Silva, R., Vongsanga, K., Wang, X. & Byrne, N. Development of a novel re-generated cellulose composite material. *Carbohydr. Polym.* **121**, 382–387 (2015).

62. Abbott, A. P., Boothby, D., Capper, G., Davies, D. L. & Rasheed, R. K. Deep Eutectic Solvents formed between choline chloride and carboxylic acids: Versatile alternatives to ionic liquids. *J. Am. Chem. Soc.* **126**, 9142–9147 (2004).

63. Smith, E. L., Abbott, A. P. & Ryder, K. S. Deep Eutectic Solvents (DESs) and Their Applications. *Chem. Rev.* **114**, 11060–11082 (2014).

64. Wahlström, R., Rommi, K., Willberg-Keyriläinen, P., Ercili-Cura, D., Holopainen-Mannila, U., Hiltunen, J., Mäkinen, O., Nygren, H., Mikkelson, A. & Kuutti, L. High Yield Protein Extraction from Brewer's Spent Grain with Novel Carboxylate Salt - Urea Aqueous Deep Eutectic Solvents. *ChemistrySelect* **2**, 9355–9363 (2017).

65. Sirviö, J. A., Visanko, M. & Liimatainen, H. Deep eutectic solvent system based on choline chloride-urea as a pre-treatment for nanofibrillation of wood cellulose. *Green Chem.* **17**, 3401–3406 (2015).

66. Tenhunen, T., Lewandowska, A., Orelma, H., Johansson, L., Virtanen, T., Harlin, A., Österberg, M., Eichhorn, S. & Tammelin, T. Understanding the interactions of cellulose fibres and deep eutectic solvent of choline chloride and urea. *Cellulose* **25**, 137–150 (2018).

67. Willberg-Keyriläinen, P., Hiltunen, J. & Ropponen, J. Production of cellulose carbamate using urea-based deep eutectic solvents. *Cellulose* **25**, 195–204 (2018).

68. Moore, K. E., Mangos, D. N., Slattery, A. D., Raston, C. L. & Boulos, R. A. Wool deconstruction using a benign eutectic melt. *RSC Adv.* **6**, 20095–20101 (2016).

69. Jiang, Z., Yuan, J., Wang, P., Fan, X., Xu, J., Wang, Q. & Zhang, L. Dissolution and regeneration of wool keratin in the deep eutectic solvent of choline chloride-urea. *Int. J. Biol. Macromol.* **119**, 423–430 (2018).

70. Wang, D. & Tang, R. C. Dissolution of wool in the choline chloride/oxalic acid deep eutectic solvent. *Mater. Lett.* **231**, 217–220 (2018).

71. Singh, H. & MacRitchie, F. Application of polymer science to properties of gluten. *J. Cereal Sci.* **33**, 231–243 (2001).

72. Patterson, D. Free Volume and Polymer Solubility. A Qualitative View. *Macromolecules* **2**, 672–677 (1969).

73. Blanks, R. F. & Prausnitz, J. M. Thermodynamics of polymer solubility in polar and nonpolar systems. *Ind. Eng. Chem.* **56**, 67 (1964).

74. Holmberg, K., Jönsson, B., Kronberg, B. & Lindman, B. Surfactants and Polymers in Aqueous Solution. 2nd edition. 527 *John Wiley & Sons Ltd* (2004). ISBN 0-471-49883-1

75. Schein, C. H. Solubility as a function of protein structure and solvent components. *NatureBio/technology* **8**, 308–317 (1990).

76. van Oss, C. J., Good, R. J. & Chaudhury, M. K. Solubility of proteins. *J. Protein Chem.* **5**, 385–405 (1986).

77. Bennion, B. J. & Daggett, V. The molecular basis for the chemical denaturation of proteins by urea. *Proc. Natl. Acad. Sci. U. S. A.* **100**, 5142–5147 (2003).

78. Dalev, P. G. Utilisation of waste feathers from poultry slaughter for production of a protein concentrate. *Bioresour. Technol.* **48**, 265–267 (1994).

79. Eslahi, N., Hemmatinejad, N. & Dadashian, F. From feather waste to valuable nanoparticles. *Part. Sci. Technol.* **32**, 242–250 (2014).

80. Rocha Plácido Moore, G., Maria Martelli, S., Gandolfo, C., José do Amaral Sobral, P. & Borges Laurindo, J. Influence of the glycerol concentration on some physical properties of feather keratin films. *Food Hydrocoll.* **20**, 975–982 (2006).

81. Nagai, Y. & Nishikawa, T. Alkali Solubilization of Chichken Feather Keratin. *Agric. Biol. Chem.* **34**, 16–22 (1970).

82. Zhao, W., Yang, R., Zhang, Y. & Wu, L. Sustainable and practical utilization of feather keratin by an innovative physicochemical pretreatment: High density steam flash-explosion. *Green Chem.* **14**, 3352–3360 (2012).

83. Zhao-Tie, L., Ping, S. & Zhong-Wen, L. Chemically modified chicken feather as sorbent for removing toxic chromium(VI) ions. *Ind. Eng. Chem. Res.* **48**,

6882–6889 (2009).

84. Khosa, M. A., Wu, J. & Ullah, A. Chemical modification, characterization, and application of chicken feathers as novel biosorbents. *RSC Adv.* **3**, 20800–20810 (2013).

85. Harrap, B. S. & Woods, E. F. Soluble Derivatives of Feather Keratin. *Biochem. J.* **92**, 8–18 (1964).

86. Chan, K. Y. & Wasserman, B. P. Direct Colorimetric Assay of Free Thiol-Groups and Disulfide Bonds in Suspensions of Solubilized and Particulate Cereal Proteins. *Cereal Chem.* **70**, 22–26 (1993).

87. Woodin, A. M. Molecular size, shape and aggregation of soluble feather keratin. *Biochem. J.* **57**, 99–109 (1954).

88. Gurkovskaya, E. A. Thin-layer size-exclusion chromatography of polymers. *Russ. J. Appl. Chem.* **81**, 360–369 (2008).

89. Caprioli, R. M., Farmer, T. B. & Gile, J. Molecular Imaging of Biological Samples: Localization of Peptides and Proteins Using MALDI-TOF MS. *Anal. Chem.* **69**, 4751–4760 (1997).

90. Hu, X., Cebe, P., Weiss, A. S., Omenetto, F. & Kaplan, D. L. Protein-based composite materials. *Mater. Today* **15**, 208–215 (2012).

91. Ma, B., Qiao, X., Hou, X. & Yang, Y. Pure keratin membrane and fibers from chicken feather. *Int. J. Biol. Macromol.* **89**, 614–621 (2016).

92. Barth, A. Infrared spectroscopy of proteins. *Biochim. Biophys. Acta - Bioenerg.* **1767**, 1073–1101 (2007).

93. Tsuboi, M., Kaneuchi, F., Teruki, I. & Akahane, K. Infrared and Raman micoroscopy of fowl feather barb. *Can. J. Chem.* **69**, 1752–1757 (1991).

94. Rintoul, L., Carter, E. A., Stewart, S. D. & Fredericks, P. M. Keratin orientation in wool and feathers by polarized Raman spectroscopy. *Biopolym. - Biospectroscopy Sect.* **57**, 19–28 (2000).

95. Duer, M. J., McDougal, N. & Murray, R. C. A solid-state NMR study of the structure and molecular mobility of α-keratin. *Phys. Chem. Chem. Phys.* **5**, 2894–2899 (2003).

96. Yao, W., Weng, Y. & Catchmark, J. M. Improved cellulose X-ray diffraction analysis using Fourier series modeling. *Cellulose* **27**, 5563–5579 (2020).

97. Terinte, N., Ibbett, R. & Schuster, K. C. Overview on native cellulose and microcrystalline cellulose I structure studied by X-ray diffraction (WAXD): Comparison between measurement techniques. *Lenzinger Berichte* **89**, 118–131 (2011).

98. Kim, S. H., Lee, C. M. & Kafle, K. Characterization of crystalline cellulose in biomass: Basic principles, applications, and limitations of XRD, NMR, IR, Raman, and SFG. *Korean J. Chem. Eng.* **30**, 2127–2141 (2013).

99. Hu, C., Reddy, N., Yan, K. & Yang, Y. Acetylation of chicken feathers for thermoplastic applications. *J. Agric. Food Chem.* **59**, 10517–10523 (2011).

100. Reddy, N., Chen, L. & Yang, Y. Biothermoplastics from hydrolyzed and citric acid Crosslinked chicken feathers. *Mater. Sci. Eng. C* **33**, 1203–1208 (2013).

101. Dou, Y., Zhang, B., He, M., Yin, G. & Cui, Y. The structure, tensile properties and water resistance of hydrolyzed feather keratin-based bioplastics. *Chinese J. Chem. Eng.* **24**, 415–420 (2016).

102. Song, N., Jo, W., Song, H., Chung, K., Won, M. & Song, K. Effects of plasticizers and nano-clay content on the physical properties of chicken feather protein composite films. *Food Hydrocoll.* **31**, 340–345 (2013).

103. Poole, A. J. & Church, J. S. The effects of physical and chemical treatments on Na2S produced feather keratin films. *Int. J. Biol. Macromol.* **73**, 99–108 (2015).

104. Schrooyen, P. M. M., Dijkstra, P. J., Oberthür, R. C., Bantjes, A. & Feijen, J. Partially carboxymethylated feather keratins. 2. Thermal and mechanical properties of films. *J. Agric. Food Chem.* **49**, 221–230 (2001).

105. Wihodo, M. & Moraru, C. I. Physical and chemical methods used to enhance the structure and mechanical properties of protein films: A review. *J. Food Eng.* **114**, 292–302 (2013).

106. Ramakrishnan, N., Sharma, S., Gupta, A. & Alashwal, B. Y. Keratin based bioplastic film from chicken feathers and its characterization. *Int. J. Biol. Macromol.* **111**, 352–358 (2018).

107. Martelli, S. M., Moore, G. R. P. & Laurindo, J. B. Mechanical properties, water vapor permeability and water affinity of feather keratin films plasticized with sorbitol. *J. Polym. Environ.* **14**, 215–222 (2006).

108. Martelli, S. M., Moore, G., Silva Paes, S., Gandolfo, C. & Laurindo, J. B. Influence of plasticizers on the water sorption isotherms and water vapor permeability of chicken feather keratin films. *LWT - Food Sci. Technol.* **39**, 292–301 (2006).

109. Martelli, S. M. & Laurindo, J. B. Chicken feather keratin films plasticized with polyethylene glycol. *Int. J. Polym. Mater. Polym. Biomater.* **61**, 17–29 (2012).

110. Marquié, C. Chemical reactions in cottonseed protein cross-linking by formaldehyde, glutaraldehyde, and glyoxal for the formation of protein films with enhanced mechanical properties. *J. Agric. Food Chem.* **49**, 4676–4681 (2001).

111. Park, S. K., Bae, D. H. & Rhee, K. C. Soy protein biopolymers cross-linked with glutaraldehyde. *J. Am. Oil Chem. Soc.* **77**, 879–884 (2000).

112. Tanabe, T., Okitsu, N. & Yamauchi, K. Fabrication and characterization of chemically crosslinked keratin films. *Mater. Sci. Eng. C* **24**, 441–446 (2004).

113. Uranga, J., Leceta, I., Etxabide, A., Guerrero, P. & De La Caba, K. Cross-linking of fish gelatins to develop sustainable films with enhanced properties. *Eur. Polym. J.* **78**, 82–90 (2016).

114. Bigi, A., Cojazzi, G., Panzavolta, S., Rubini, K. & Roveri, N. Mechanical and thermal properties of gelatin films at different degrees of glutaraldehyde crosslinking. *Biomaterials* **16**, 1964-1973.e1 (2018).

115. González, A., Strumia, M. C. & Alvarez Igarzabal, C. I. Cross-linked soy protein as material for biodegradable films: Synthesis, characterization and biodegradation. *J. Food Eng.* **106**, 331–338 (2011).

116. Vernon-Parry, K. D. Scanning Electron Microscopy : an introduction. *Analysis* **13**, 40–44 (2000).

117. Gennadios, A., Brandenburg, A. H., Park, J. W., Weller, C. L. & Testin, R. F. Water vapor permeability of wheat gluten and soy protein isolate films. *Ind. Crops Prod.* **2**, 189–195 (1994).

118. Shogren, R. Water vapor permeability of biodegradable polymers. *J. Environ. Polym. Degrad.* **5**, 91–95 (1997).

119. Farris, S., Introzzi, L., Biagioni, P., Holz, T., Schiraldi, A. & Piergiovanni, L. Wetting of biopolymer coatings: Contact angle kinetics and image analysis investigation. *Langmuir* **27**, 7563–7574 (2011).

120. Tran, C. D., Prosencyes, F., Franko, M. & Benzi, G. Synthesis, structure and antimicrobial property of green composites from cellulose, wool, hair and chicken feather. *Carbohydr. Polym.* **151**, 1269–1276 (2016).

121. De Silva, R., Wang, X. & Byrne, N. Development of a novel cellulose/duck feather composite fibre regenerated in ionic liquid. *Carbohydr. Polym.* **153**, 115–123 (2016).

122. Grigsby, W. J., Scott, S. M., Plowman-holmes, M. I., Middlewood, P. G. & Recabar, K. Acta Biomaterialia Combination and processing keratin with lignin as biocomposite materials for additive manufacturing technology. *Acta Biomater.* **104**, 95–103 (2020).

123. Kontturi, E., Tammelin, T. & Österberg, M. Cellulose—model films and the fundamental approach. *Chem. Soc. Rev.* **35**, 1287–1304 (2006).

124. Kontturi, E., Thüne, P. C. & Niemantsverdriet, J. W. Novel method for preparing cellulose model surfaces by spin coating. *Polymer (Guildf).* **44**, 3621–3625 (2003).

125. Kontturi, E., Thüne, P. C. & Niemantsverdriet, J. W. Cellulose model surfaces-simplified preparation by spin coating and characterization by X-ray photoelectron spectroscopy, infrared spectroscopy, and atomic force microscopy. *Langmuir* **19**, 5735–5741 (2003).

126. Holmberg, M., Berg, J., Stemme, S., Ödberg, L., Rasmusson, J. & Claesson, P. Surface Force Studies of Langmuir – Blodgett Cellulose Films. *J. Colloid Interface Sci.* **186**, 369–381 (1997).

127. Schaub, M., Wenz, G., Wegner, G. & Sfein, A. Ultrathin Films of Cellulose on Silicon Wafers. *Adv. Mater.* **5**, 919–922 (1993).

128. Tammelin, T., Österberg, M., Johansson, L. S. & Laine, J. Preparation of lignin

and extractive model surfaces by using spincoattng technique - Application for QCM-D studies. *Nord. Pulp Pap. Res. J.* **21**, 444–450 (2006).

129. Farooq, M., Zou, T., Valle-Delgado, J., Sipponen, M., Morits, M. & Österberg, M. Well-Defined Lignin Model Films from Colloidal Lignin Particles. *Langmuir* **36**, 15592–15602 (2020).

130. Reviakine, I., Johannsmann, D. & Richter, R. P. Hearing what you cannot see and visualizing what you hear: Interpreting quartz crystal microbalance data from solvated interfaces. *Anal. Chem.* **83**, 8838–8848 (2011).

131. Sauerbrey, G. Verwendung von Schwingquarzen zur Wägung dünner Schichten und zur Mikrowägung*. *Zeitschrift für Phys.* **155**, 206–222 (1959).

132. Höök, F., Rodahl, M., Brzezinski, P. & Kasemo, B. Energy Dissipation Kinetics for Protein and Antibody - Antigen Adsorption under Shear Oscillation on a Quartz Crystal Microbalance. *Langmuir* **7463**, 729–734 (1998).

133. Naderi, A. & Claessont, P. M. Adsorption properties of polyelectrolyte-surfactant complexes on hydrophobic surfaces studied by QCM-D. *Langmuir* **22**, 7639–7645 (2006).

134. Siow, K. S., Britcher, L., Kumar, S. & Griesser, H. J. QCM-D and XPS study of protein adsorption on plasma polymers with sulfonate and phosphonate surface groups. *Colloids Surfaces B Biointerfaces* **173**, 447–453 (2019).

135. Dutta, A. K., Nayak, A. & Belfort, G. Viscoelastic properties of adsorbed and cross-linked polypeptide and protein layers at a solid-liquid interface. *J. Colloid Interface Sci.* **324**, 55–60 (2008).

136. Salas, C., Rojas, O. J., Lucia, L. A., Hubbe, M. A. & Genzer, J. Adsorption of glycinin and β-conglycinin on silica and cellulose: Surface interactions as a function of denaturation, pH, and electrolytes. *Biomacromolecules* **13**, 387–396 (2012).

137. Orelma, H., Filpponen, I., Johansson, L. S., Laine, J. & Rojas, O. J. Modification of cellulose films by adsorption of cmc and chitosan for controlled attachment of biomolecules. *Biomacromolecules* **12**, 4311–4318 (2011).

138. Leskinen, T., Witos, J., Valle-Delgado, J., Lintinen, K., Kostiainen, M., Wiedmer, S., Österberg, M. & Mattinen, M. Adsorption of Proteins on Colloidal Lignin Particles for Advanced Biomaterials. *Biomacromolecules* **18**, 2767–2776 (2017).

139. Strasser, S., Niegelhell, K., Kaschowitz, M., Markus, S., Kargal, R., Stana-Kleinschek, K., Slugovc, C., Mohan, T. & Spirk, S. Exploring Nonspecific Protein Adsorption on Lignocellulosic Amphiphilic Bicomponent Films. *Biomacromolecules* **17**, 1083–1092 (2016).

140. Salas, C., Rojas, O. J., Lucia, L. A., Hubbe, M. A. & Genzer, J. On the surface interactions of proteins with lignin. *ACS Appl. Mater. Interfaces* **5**, 199–206 (2013).

141. Nakanishi, K., Sakiyama, T. & Imamura, K. On the Adsorption of Proteins on Solid Surfaces , a Common but Very Complicated Phenomenon. *Journal of Bioscience and Bioengineering*. **91**, 233–244 (2001).

142. Norde, W. Protein adsorption at solid surfaces: A thermodynamic approach. *Pure Appl. Chem.* **66**, 491–496 (1994).

143. Norde, W. My voyage of discovery to proteins in flatland . . . and beyond. *Colloids Surfaces B Biointerfaces* **61**, 1–9 (2008).

144. Malmsten, M. Biopolymers at Interfaces. 2nd edition. 672, *Marcel Dekker, Inc.* (2005). ISBN 0-203-91200-4

145. Arai, T. & Norde, W. The behavior of some model proteins at solid-liquid interfaces 1 . Adsorption from single protein solutions. *Colloids and Surfaces* **51**, 1–15 (1990).

146. Yamaguchi, A., Isozaki, K., Nakamura, M., Takaya, H. & Watanabe, T. Discovery of 12-mer peptides that bind to wood lignin. *Sci. Rep.* **6**, 1–11 (2016).

147. Mohan, T., Niegelhell, K. Zarth, C., Kargl, R., Köstler, S., Ribitsch, V., Heinze, T., Spirk, S. & Stana-Kleinschek, K. Triggering protein adsorption on tailored cationic cellulose surfaces. *Biomacromolecules* **15**, 3931–3941 (2014).

148. Khakalo, A., Filpponen, I. & Rojas, O. J. Protein Adsorption Tailors the Surface Energies and Compatibility between Polylactide and Cellulose Nanofibrils. *Biomacromolecules* **18**, 1426–1433 (2017).

149. Fang, W., Paananen, A., Vitikainen, M., Koskela, S., Westerholm-Parvonen, A., Joensuu, J., Landowski, C., Penttilä, M., Linder, M. & Laaksonen, P. Elastic and pH-Responsive Hybrid Interfaces Created with Engineered Resilin and Nanocellulose. *Biomacromolecules* **18**, 1866–1873 (2017).

150. Cao, J. & Billows, C. A. Crystallinity determination of native and stretched wool by X-ray diffraction. *Polym. Int.* **48**, 1027–1033 (1999).

151. Ghosh, A., Clerens, S., Deb-Choudhury, S. & Dyer, J. M. Thermal effects of ionic liquid dissolution on the structures and properties of regenerated wool keratin. *Polym. Degrad. Stab.* **108**, 108–115 (2014).

152. Wang, D., Yang, X. H., Tang, R. C. & Yao, F. Extraction of keratin from rabbit hair by a deep eutectic solvent and its characterization. *Polymers (Basel).* **10**, (2018).

153. Swatloski, R. P., Spear, S. K., Holbrey, J. D. & Rogers, R. D. Dissolution of cellose with ionic liquids. *J. Am. Chem. Soc.* **124**, 4974–4975 (2002).

154. Sharma, S., Gupta, A., Chik, S., Kee, C., Mistry, B., Kim, D. & Sharma, G. Characterization of keratin microparticles from feather biomass with potent antioxidant and anticancer activities. *Int. J. Biol. Macromol.* **104**, 189–196 (2017).

155. Sun, N., Rahman, M., Qin, Y., Maxim, M., Rodríguez, H. & Rogers, R. Complete dissolution and partial delignification of wood in the ionic liquid 1-ethyl-3-methylimidazolium acetate. *Green Chem.* **11**, 646–655 (2009).

156. Parnica, J. & Antalik, M. Urea and guanidine salts as novel components for deep eutectic solvents. *J. Mol. Liq.* **197**, 23–26 (2014).

157. Monhemi, H., Housaindokht, M. R., Moosavi-Movahedi, A. A. & Bozorgmehr, M. R. How a protein can remain stable in a solvent with high content of urea: Insights from molecular dynamics simulation of Candida antarctica lipase B in urea: Choline chloride deep eutectic solvent. *Phys. Chem. Chem. Phys.* **16**, 14882–14893 (2014).

158. Stockmayer, W. H. Solubility of heterogeneous polymers. *J. Chem. Phys.* **17**, 588 (1949).

159. Sakellariou, P., Abraham, M. H. & Whiting, G. S. Solubility characteristics of poly(ethylene oxide): Effect of molecular weight, end groups and temperature. *Colloid Polym. Sci.* **272**, 872–875 (1994).

160. Reddy, N., Jiang, Q. & Yang, Y. Preparation and properties of peanut protein films crosslinked with citric acid. *Ind. Crops Prod.* **39**, 26–30 (2012).

161. Martucci, J. F., Accareddu, A. E. M. & Ruseckaite, R. A. Preparation and characterization of plasticized gelatin films cross-linked with low concentrations of Glutaraldehyde. *J Mater Sci.* **47** 3282–3292 (2012).

162. Dou, Y., Huang, X., Zhang, B., He, M., Yin, G. & Cui, Y. Preparation and characterization of a dialdehyde starch crosslinked feather keratin film for food packaging application. *RSC Adv.* **5**, 27168–27174 (2015).

163. McHugh, T. H. & Krochta, J. M. Sorbitol-vs Glycerol-Plasticized Whey Protein Edible Films: Integrated Oxygen Permeability and Tensile Property Evaluation. *J. Agric. Food Chem.* **42**, 841–845 (1994).

164. Martucci, J. F., Espinosa, J. P. & Ruseckaite, R. A. Physicochemical Properties of Films Based on Bovine Gelatin Cross-linked with 1,4-Butanediol Diglycidyl Ether. *Food Bioprocess Technol.* **8**, 1645–1656 (2015).

165. Xu, F., Zhang, W., Zhang, S., Li, L., Li, J. & Zhang, Y. Preparation and characterization of poly(vinyl alcohol) and 1,2,3-propanetriol diglycidyl ether incorporated soy protein isolate-based films. *J. Appl. Polym. Sci.* **132**, 1–8 (2015).

166. Migneault, I., Dartiguenave, C., Bertrand, M. J. & Waldron, K. C. Glutaraldehyde: behavior in aqueous solution, reaction with proteins, and application to enzyme crosslinking. *Biotechniques* **37**, 18687–18705 (2004).

167. Johnson, L. F., Schwartz, I. L. & Walter, R. Oxytocin and neurohypophyseal peptides: spectral assignment and conformational analysis by 220 MHz nuclear magnetic resonance. *Biochemistry* **64**, 1269–1275 (1969).

168. Ustunol, Z. & Mert, B. Water solubility, mechanical, barrier, and thermal properties of cross-linked whey protein isolate-based films. *J. Food Sci.* **69**, (2004).

169. Vilchez, V., Dieckmann, E., Tammelin, T., Cheeseman, C. & Lee, K. Y. Upcycling Poultry Feathers with (Nano)cellulose: Sustainable Composites Derived from Nonwoven Whole Feather Preforms. *ACS Sustain. Chem. Eng.* **8**, 14263–

14267 (2020).

170. Dieckmann, E., Eleftheriou, K., Audic, T., Lee, K-Y., Sheldrick, L. & Cheeseman, C. New sustainable materials from waste feathers: Properties of hot-pressed feather/cotton/bi-component fibre boards. *Sustain. Mater. Technol.* **20**, e00107 (2019).

171. Elschner, T., Bračič, M., Mohan, T., Kargl, R. & Stana Kleinschek, K. Modification of cellulose thin films with lysine moieties: a promising approach to achieve antifouling performance. *Cellulose* **25**, 537–547 (2018).

172. Tammelin, T., Saarinen, T., Österberg, M. & Laine, J. Preparation of Langmuir/Blodgett-cellulose surfaces by using horizontal dip- ping procedure. Application for polyelectrolyte adsorption studies performed with QCM-D. *Cellulose* **13**, 519–535 (2006).

173. Sipponen, M. H., Smyth, M., Leskinen, T., Johansson, L. & Österberg, M. lignin particles: stabilization of durable Pickering emulsions †. *Green Chem.* **19**, 5831–5840 (2017).

174. Boraston, A. B., Bolam, D. N., Gilbert, H. J. & Davies, G. J. Carbohydrate-binding modules: Fine-tuning polysaccharide recognition. *Biochem. J.* **382**, 769–781 (2004).

175. Dee, K. C., Puleo, D. A. & Bizios, R. An Introduction to Tissue-Biomaterial Interactions. 248 *Wiley* (2002). ISBN: 978-0-471-25394-5

**BUSINESS +
ECONOMY**

**ART +
DESIGN +
ARCHITECTURE**

**SCIENCE +
TECHNOLOGY**

CROSSOVER

**DOCTORAL
THESES**